

Glaciotectonic deformation and reinterpretation of the Worth Point stratigraphic sequence: Banks Island, NT, Canada

Jessica M. Vaughan^a, John H. England^a and David J.A. Evans^b

^a University of Alberta, Edmonton, AB T6G 2R3, Canada

^b Durham University, Durham City, County Durham, England DH1 3LE, UK

Hill-hole pairs, comprising an ice-pushed hill and associated source depression, cluster in a belt along the west coast of Banks Island, NT. Ongoing coastal erosion at Worth Point, southwest Banks Island, has exposed a section (6 km long and w30 m high) through an ice-pushed hill that was transported w 2 km from a corresponding source depression to the southeast. The exposed stratigraphic sequence is polydeformed and comprises folded and faulted rafts of Early Cretaceous and Late Tertiary bedrock, a prominent organic raft, Quaternary glacial sediments, and buried glacial ice. Three distinct structural domains can be identified within the stratigraphic sequence that represent proximal to distal deformation in an ice-marginal setting. Complex thrust sequences, interfering fold-sets, brecciated bedrock and widespread shear structures superimposed on this ice-marginally deformed sequence record subsequent deformation in a subglacial shear zone. Analysis of cross-cutting relationships within the stratigraphic sequence combined with OSL dating indicate that the Worth Point hill-hole pair was deformed during two separate glaciotectonic events. Firstly, ice sheet advance constructed the hill-hole pair and glaciotectonized the strata ice-marginally, producing a proximal to distal deformation sequence. A glacioisostatically forced marine transgression resulted in extensive reworking of the strata and the deposition of a glaciomarine diamict. A readvance during this initial stage reformed the strata in a subglacial shear zone, overprinting complex deformation structures and depositing a glaciotectonite w20 m thick. Outwash channels that incise the subglacially deformed strata record a deglacial marine regression, whereas aggradation of glaciofluvial sand and gravel infilling the channels record a subsequent marine transgression. Secondly, a later, largely non-erosive ice margin overrode Worth Point, deforming only the most surficial units in the section and depositing a capping till. The investigation of the Worth Point stratigraphic sequence provides the first detailed description of the internal architecture of a polydeformed hill-hole pair, and as such provides an insight into the formation and evolution of an enigmatic landform. Notably, the stratigraphic sequence documents icemarginal and subglacial glaciotectonics in permafrost terrain, as well as regional glacial and relative sea level histories. The reinterpreted stratigraphy fundamentally rejects the long-established paleoenvironmental history of Worth Point that assumed a simple 'layer-cake' stratigraphy including the typesite for an organically rich, preglacial interval (Worth Point Fm).

1. Introduction

Previous investigations of Neogene and Quaternary deposits preserved at the surface and within purportedly in situ subsurface sections across Banks Island proposed the lengthiest framework of environmental change in the Canadian Arctic Archipelago (CAA; Vincent, 1982, 1983, 1989, 1990; Vincent et al., 1983, 1984; Barendregt et al., 1998). The framework documented up to eight continental glaciations and five interglaciations associated with multiple marine transgression/regression cycles that span the entire Pleistocene (Vincent et al., 1984; Vincent, 1990; Barendregt et al., 1998). Stratigraphic units exposed at Worth Point, southwest Banks Island, form a critical type section reported to include a 'layer-cake' sequence of preglacial organics assigned to the Worth Point Fm, till from the earliest glaciation on Banks Island, and marine deposits from a glacioisostatically forced marinetransgression during an intermediate glaciation (Vincent, 1982, 1983, 1984, 1989, 1990, 1992; Vincent et al., 1984; Matthews et al., 1986; Barendregt et al., 1998). Magnetostratigraphic analyses of the Pleistocene units identified the BruhnesMatuyama magnetic

reversal (0.78 Ma) at the contact between the Worth Point Fm and overlying till, forming an important marker horizon that permitted long distance correlations between the Banks Island framework, magnetically constrained Arctic Ocean records, and widespread North American Quaternary marine and terrestrial records (Clark et al., 1984; Barendregt et al., 1998; Darby, 2003; Ehlers and Gibbard, 2004; Ehlers et al., 2011). This paper directly tests this elaborate and influential model. Recently, the integrity of the Banks Island environmental framework has been challenged by a fundamental revision of the surficial geology of Banks Island (England et al., 2009; Lakeman and England, 2012, 2013). This research amalgamates all of the former multiple Quaternary till sheets (assigned to three glaciations, Vincent, 1982) into a single, island-wide Late Wisconsinan glaciation (England et al., 2009; Lakeman and England, 2013). Consequently, this revised surficial model on Banks Island warrants the reinvestigation of the subsurface stratigraphy, whose events were assumed to mirror those of the previous, multiple glaciation model, including their proposed pre and postglacial seas and intervening interglacials.

New investigations of the stratigraphy at Worth Point indicate that the deposits are pervasively glaciotectionized, thereby contradicting the previously proposed 'layer-cake' stratigraphy and implicitly their former palaeoenvironmental interpretations. This paper presents the sedimentology, structural geology and chronology of the Worth Point section and provides a revised architectural framework that constitutes the first detailed reconstruction of glaciotectionism on Banks Island, CAA (Figs. 1 and 2).

1.1. Objectives and methods

The objectives of this paper are: (1) to describe the geomorphology, stratigraphy, sedimentology, glaciotectionic architecture and deformation structures at Worth Point; (2) to reconstruct the glacial stress regimes responsible for glaciotectionism and to differentiate between deformation in proglacial, ice-marginal and subglacial environments; (3) to determine the number of glaciotectionic events responsible for deformation at Worth Point and their relative and absolute chronology, and; (4) to determine the role of permafrost in facilitating glaciotectionism and influencing the style and magnitude of deformation. These objectives are achieved through a multidisciplinary approach combining geomorphology, stratigraphy, sedimentology and structural analyses. Separate lithologic units are identified and described according to grain size, sorting, depositional structures, deformation structures, inclusions, and degree of consolidation and lithification. The tectonostratigraphy of the bluffs is constructed based on lithostratigraphy, lithofacies boundaries, contacts and shear zones, the style of deformation (ductile or brittle) and the orientation of folds and faults. Specific attention is given to analysing cross-cutting relationships and overprinted deformation structures in order to reconstruct the relative timing of tectonic events. The range of macro-scale deformation structures and their size, frequency and orientation are recorded. Four sections were selected to be logged in detail, each representative of a primary and diagnostic deformation style. Clast form and macrofabric analyses, as well as thin section analysis, were undertaken to discriminate between former depositional/deformational styles and environments. Absolute chronological control for the deposition of key glacial deposits was established through the employments of OSL dating (e.g. Wintle, 2010) and relative chronological control was established through the analysis of cross-cutting and overprinted deformation structures.

1.2. Regional setting

The coast of southwest Banks Island is subject to widespread slope failure and erosion due to ongoing submergence, enhanced coastal erosion as summer sea ice is reduced, and the melt-out of permafrost and buried glacial ice (Fig. 3a and b). The landscape is characterized by low arctic tundra inset by large river valleys draining westward to the Beaufort Sea across gently undulating terrain. Meltwater channels, small recessional moraines, and glaciotectionized landforms related to the former passage and wastage of Laurentide ice dominate the glacial geomorphology. Ice-pushed hills

flanking the west coast of Banks Island are the most common glaciotectonic landforms, forming distinct topographic highs displaced by the westward flowing Laurentide Ice Sheet (LIS). The ice pushed hill at Worth Point is mildly crescentic in shape with tectonized ridges forming the crest. The hill is associated with a similarly-sized depression directly inland (southeast) occupied by two lakes and adjacent tundra ponds, thought to mark the source depression (Fig. 2). Numerous coastal bluffs expose a detailed record of widely-correlated glacial and nonglacial Quaternary environments (Vincent, 1990; Barendregt et al., 1998).

2. Results

Due to the detailed descriptions of complex lithofacies and deformation structures presented in the following section, important sedimentological and stratigraphical interpretations are made throughout to aid the reader. The sedimentology of eight lithofacies identified in the Worth Point stratigraphic sequence are presented and interpreted first. Interpreted lithologic units are then placed into the broader context of the tectonic architecture at Worth Point. This architecture is subdivided into three major structural domains, A- C, from south to north. Each structural domain is presented and interpreted separately, with a representative section from each domain logged and described in detail to better characterize local deformation styles within dominant lithologic units. Finally, section-wide deformation structures are presented and interpreted in their spatial and stratigraphic context.

2.1. Sedimentology

Eight lithofacies are identified in the glaciotectonized Worth Point stratigraphic sequence. Original lithofacies thickness, geometry, and contacts remain unknown due to extensive deformation.

2.1.1. Lithofacies 1: laminated mudstone (Late Cretaceous Kanguk Formation e Kk Fm)

LF 1 is the most exposed unit at Worth Point, extending below the base of the bluffs in many locations and occurring as stacked rafts >30 m thick (Fig. 3c). It is composed of well-sorted, dark grey brown clay displaying distinct bedding, presumably once horizontal. Individual laminae are <1 cm thick, show little internal variation and contain no inclusions or limestones. The unit reflects deposition in a stable, low-energy environment, most likely distal marine. LF 1 is interpreted to be distal marine mudstones of the Late Cretaceous Kanguk Formation (Kk Fm). Comparable outcrops of mudstone assigned to the Kk Fm have been widely observed throughout the Canadian Arctic (Núñez-Betelu et al., 1994).

2.1.2. Lithofacies 2: cobble-gravel, sandstone and siltstone with compressed organics (Palaeocene-Eocene Eureka Sound Formation (ES Fm))

LF 2 occurs as discrete rafts that are most common in the southern and central parts of the Worth Point stratigraphic sequence (Fig. 3d). It includes well-sorted, fining-upwards sequences of horizontally-bedded, quartzite-dominated cobble-gravel, imbricated granules-cobbles, cross-bedded granules and sand, silt, and flaser-bedded clay. The unit is semi-lithified to unlithified with compressed charcoal inclusions throughout. The most commonly exposed components of the fining-upwards sequence are cross-bedded silt and sand that have been stained green and red by presumed groundwater seepage. The sequence reflects deposition in a deltaic environment with channel, bar, overbank, and tidal deposits. LF 2 is interpreted to be the low-energy deltaic deposits of the Paleocene-Eocene Eureka Sound Formation (ES Fm). Comparable cyclic successions of sand, silt, shale and lignitic coal assigned to the ES Fm have been described on northern Banks Island and throughout the Canadian Arctic (Miall, 1976).

2.1.3. Lithofacies 3: sand and gravel with uncompressed logs and organics (Pliocene Beaufort Formation e Bft Fm)

LF 3 occurs as discrete rafts and isolated pods, and has been commonly fluidized and remobilized throughout the Worth Point stratigraphic sequence (Fig. 3e). It includes unlithified, horizontally bedded and occasionally cross-bedded, well-sorted sand and gravel, cross-bedded sand, and uncompressed and waterworn logs, peat mats and disseminated organics. The gravel clasts are very rounded (RWR=68%; Fig 4, Sites 3 and 4), clast-supported, and dominated by quartzite, sandstone, and siltstone, with a noticeable lack of granite. Clast size is fairly consistent, with long-axes of 2.5-19 cm and a mode of 7 cm. Organics are unevenly dispersed throughout LF 3, but are locally concentrated, with peat mats extending laterally <20 m and containing occasional whole logs. The clast-supported, occasionally cross-bedded nature of the sand and gravel suggesting deposition in a braided river channel, with cross-bedded sand recording bar deposition and localized concentrations of organics recording the build-up of overbank vegetation in former log jams and/or the establishment of vegetation in abandoned channels. LF 3 is assigned to the Pliocene Beaufort Formation (Bft Fm). The occurrence of unaltered wood (mostly conifers) and organics, associated with horizontally-bedded and cross-bedded sand and gravel are characteristic of the Bft Fm and are consistent with other exposures described across Banks Island (Fyles et al., 1994) and elsewhere in the CAA (Tozer, 1956; Craig and Fyles, 1960).

2.1.4. Lithofacies 4: crudely stratified mudstone with lonestones (glaciomarine diamict)

LF 4 occurs as discrete rafts and is common in the central and northern section of the stratigraphic sequence (Fig. 3f). It comprises well-sorted, grey-brown clay that is compositionally similar to LF 1. However, LF 4 displays crude bedding, presumably originally horizontal. Individual beds are w10 cm thick and are visible only by a change in colour, not grain size. Small pebble-granule inclusions (<5 cm) are dispersed throughout the unit and are largely composed of quartzite and sandstone with rare granite. Distinctly larger clasts (<40 cm) are occasionally observed in the unit, and are commonly striated, associated with load structures, and composed of quartzite. To better differentiate between LF 1 and LF 4, electrical conductivity and pH analyses were undertaken on five samples of LF 1 and three samples of LF 4 from various locations along the bluffs. These analyses indicate that both units have similar pH values (LF 1 = 5.62-7.14 and LF 4 = 3.1-6.85). However, conductivity measurements indicate that LF 1 has consistently low conductivity values of 0.031-2.28 mS/cm whereas LF 4 has consistently higher values ranging from 10.3 to 16.8 mS/cm. The distinctly higher conductivity values for LF 4 may reflect enhanced porewater salinity as a result of more recent deposition (relative to LF 1) in a saline, marine environment. LF 4 is interpreted to be a glaciomarine diamict with striated dropstones, principally composed of reworked Kk Fm.

2.1.5. Lithofacies 5: unfossiliferous, coarse sand and gravel (glaciofluvial sand and gravel)

LF 5 infills incised valleys that grade to below modern sea level in the northernmost section of the stratigraphic sequence (Fig. 3g). The valleys contain sub-horizontally (and occasionally horizontally) bedded sand and gravel that are both unlithified and unfossiliferous. The gravel is clast-supported and sub-rounded (RWR = 23%; Fig. 4, Sites 5 and 6), with 15% of clasts bearing striae. The gravel is distinctly higher-caliber than in LF 3, with long-axes 10-35 cm with a mode of 22 cm. Dominant clast lithologies are quartzite, sandstone, and siltstone with occasional granite. Some small (<20 cm) beds of sand-granules are interbedded with gravel and display crude cross-bedding. Two samples from the sand-granule interbeds were collected for optically stimulated luminescence (OSL) dating at the Sheffield Centre for International Drylands Research, University of Sheffield, UK. Burial dates of 247 ± 17 ka and 407 ± 33 ka were obtained for the sand (quartz) grains using the single-aliquot technique. An age discrepancy of >150 ka between the OSL dates necessitates that one must be incorrect, as discussed in detail in Vaughan and England (in prep). Regardless, both dates support aggradation of the sand and gravel during the Mid-Pleistocene (*sensu lato*). LF 5 is interpreted to be glaciofluvial sand and gravel, based largely on the coarse, striated nature of the gravel as well as the occurrence of erratic granite clasts.

2.1.6. Lithofacies 6: compact diamict (subglacial traction till)

LF 6 occurs as fragmented pockets capping the central and northern parts of Worth Point (Fig. 3h). It includes a poorly-sorted, heterogeneous mix of clasts in a compacted silty-clay matrix. Clasts are mostly angular and sub-angular (RWR = 5%; Fig. 4, Sites 1 and 2), with 20% displaying striae. Dominant lithologies are quartzite, sandstone, and siltstone, with rare granite and gabbro clasts. A clast macrofabric reveals a distinct east-west orientation, with an S1 eigenvalue of 0.746 (Fig. 4, Site 2). LF 6 is interpreted as a subglacial traction till, due to its strong clast macrofabric, predominantly subangular clasts, far-travelled erratics and compaction.

2.1.7. Lithofacies 7: deformed and sheared heterogeneous diamict (glaciotectonite)

LF 7 is only exposed at the former type-site of the Worth Point Fm, where it includes a sheared, deformed, faulted and reworked *mélange* of LFs 1, 3 and 4 (Fig. 3i). It is exceptionally heterogeneous, with attenuated pods of stiff, coarse-grained sand and gravel and semi-continuous mats of peat, wood, and disseminated organics derived from LF 3. This has been incorporated into a deformed clayey-silt matrix derived from LFs 1 and 4. LF 7 displays localized fluidization and remobilization of LF 3 and a distinct increase in crude sub-horizontal banding upsection. LF 7 is interpreted as a glaciotectonite.

2.1.8. Lithofacies 8: banded debris-rich ice and massive ice (buried glacial ice and ground ice)

LF 8 is ubiquitous throughout the Worth Point section and comprises ice in two distinct forms: banded, debris-rich ice with striated clasts (Fig. 3j); and massive, clast-free ice (Fig. 3k). The banded, debris-rich ice is widespread in the southern and central parts of Worth Point where it occurs as isolated pods, rafts and larger tabular bodies (<30 m²) that form part of a thrust sequence with LFs 1, 2 and 3. Primary lithologies of debris within the ice are quartzite and sandstone derived from LF 2 and LF 3 as well as occasional ice-transported mafic and granite erratics. Debris within the ice ranges in size from mud to boulders (long axes < 40 cm) and clasts commonly display striae. Individual bands of debris range from 1 to 15 cm thickness. This ice is interpreted as buried glacial ice containing far-travelled erratics from at least southeast Banks Island as well as the Precambrian Shield on the Canadian mainland. The clast-free massive ice is also common throughout Worth Point where it tends to infill gaps and fault planes (usually < 1 m thick) rather than forming rafts and tabular bodies. This clast-free ice is interpreted to be non-glacial, epigenetic or syngenetic ground ice (Mackay, 1971, 1989).

These eight lithofacies collectively represent the primary stratigraphic units at Worth Point and are now presented in their tectonostratigraphic setting.

2.2. Tectonostratigraphy

The Worth Point stratigraphic sequence can be subdivided into three distinct structural domains (A-C) extending from south to north (Fig. 5). Each domain records a change in the intensity and style of deformation.

2.2.1. Domain A

Domain A forms the southernmost 2 km of Worth Point and is characterized by stacked, imbricated rafts of Kk Fm, ES Fm and Bft Fm (Fig. 5). Individual rafts tend to be composed of discrete bedrock units, suggesting that bedrock contacts acted as *décollement* planes. The imbricately stacked rafts are orientated towards 120° and are cross-cut toward the modern surface by bedrock rafts orientated towards 280°. The dominant dip direction towards 120° likely represents the primary direction of deformation, recording an SE-NW orientated stress field. Rafts demonstrating a crosscutting dip direction towards 280° are interpreted to record the development of conjugate shears due to the buildup of back stress. The dip of the thrust-faulted rafts progressively diminishes with elevation. For example, at the base of the bluffs, rafts dip at 50-80° whereas at the surface dips

range from near horizontal to 30° (Fig. 5). The steeper thrust angles at the base of the cliff are attributed to the presence of permafrost (at least in patches) during deformation. Permafrost would have preserved the structural integrity of each unit, permitting strata to maintain a near vertical orientation while withstanding compression and lateral compaction. Deformation becomes progressively more ductile towards Domain B (northward) where Kk Fm is the dominant lithofacies - indeed often the only material exposed for hundreds of metres.

Throughout Domain A, dense networks of faults dissect isoclinal and recumbent folds in the Kk Fm, creating rootless folds that often display drag structures (Fig. 6a and b). These folds are large-scale (amplitudes >10 m) and likely evolved from symmetric gentle and open folds to asymmetric isoclinal and recumbent folds as glacially-imposed stresses increased. Several generations of folds can be observed, with a later set of tighter overturned folds crosscutting a more open, rootless set. Disharmonic folds are widespread and indicate the onset of fold interference under a variable stress regime (Fig. 6c and d).

Throughout Domain A, the Kk Fm is heavily fragmented and dissected by a dense network of anastomosing jointing, essentially comprising a fault breccia (Fig. 3c). The distinct foliation developed during brecciation is superimposed on the bedding planes of the Kk Fm (see thin section analysis), often cross-cutting the primary bedding of the rafts but almost always paralleling the dip of the thrust-faults bounding the raft. This indicates that the shear stress field responsible for brecciation was oriented in the same direction as the previous compressional stress regime responsible for the initial displacement of the bedrock raft. The fault systems may be contemporaneous, or the same faults may have been reactivated during subsequent shear deformation. Well-defined shear zones with measurable slickensides (Fig. 7a-f) record displacement along shear planes, and indicate that the strata had significant sediment shear strength during deformation, likely reflecting the presence of permafrost.

The ES Fm forms part of the imbricate thrust sequence and is easily recognizable where it has been stained green and red by presumed groundwater seepage (Fig. 3d). Rafts of ES Fm display large-scale open folds that have been subsequently truncated by thrust-faults and reverse-faults (Fig. 8a). Elsewhere, clastic dykes are widespread throughout Domain A, testifying to the presence of liquid water and the patchy nature of permafrost (Fig. 8aec). The clastic dykes tend to comprise narrow branching networks of laminated massive sand and clay or large blow-out structures composed of coarse sand and gravel. In all cases, clastic dykes appear to have been injected into pre-existing faults and fractures, mostly along shear planes and thrusts. Because the material infilling the dykes is sourced from the host aquifer, it can be deduced that the coarse and permeable Bft Fm and ES Fm constituted the aquifers during glaciotectionism. The inclusion of cobbles, gravel, and occasional boulders (<30 cm²) within clastic dykes are testament to exceptionally high porewater pressures that fluidized the host aquifer (Rijsdijk et al., 1999). Sheared and rotated blocks of glacial ice (<10 m²) occur throughout domain A. The ice is foliated with bands of debris that occasionally bear striated clasts (Fig. 3j). It is difficult to locate the precise contact with surrounding units as the debris within the ice is dominated by Kk Fm mud that is highly susceptible to ongoing failure during melt-out. Segregated ground ice lenses and sheets that parallel the bedding of the thrust and deformed strata are also widespread. Most of this ground ice clearly formed in situ prior to deformation; nonetheless, in some sections undisturbed ground ice has preferentially developed in faults and joints after deformation (Fig. 7b).

2.2.2. Sub-domain A1

Sub-Domain A1 (Fig. 5) is located 1.2 km from the south end of Domain A where slumping has exposed an E-W orientated section (w10 m wide and w6 m high) composed of stacked rafts of Bft Fm,

ES Fm and Kk Fm (Fig. 9a). A raft of ES Fm dips at 25° towards 290° and is bounded by abrupt contacts with an overlying raft of Kk Fm and an underlying raft of Bft Fm, thereby forming an inverted sequence (i.e. the reverse order of original deposition). Because the displacement direction of the ES Fm raft is opposite to the main thrusting style observed in Domain A (orientated towards the southeast), it was likely back-thrust into position. The contact between the ES Fm and the overlying Kk Fm is characterized by numerous rip-up inclusions from the underlying ES Fm (Fig. 9b). Primary bedding structures within the ES Fm have been preserved, including flaser-bedded silt and clay overlain by compacted cobble-gravel, followed by cross-laminated sand and sandpebbles.

The excellent preservation of fine bedding within the back thrust raft of ES Fm suggests that it must have been frozen, at least in patches, during emplacement (Fig. 9b and c). Several normal faults cross-cut the compacted cobble-gravel and indicate that brittle deformation occurred within the unit before failure was accommodated at the margins by back-thrusting. A change in the style of deformation is observed toward the base of the cobble-gravel. Here, gentle anticlinal and synclinal folds occur in the cobble-gravel, and sand intrusions with load structures penetrate upward into the flaser-bedded silt and clay. This change in deformation from brittle to ductile deformation toward the base of the ES Fm raft suggests that the lower part of the ES Fm raft remained unfrozen at the time of displacement, and continued to undergo ductile deformation while overlying coarser-grained sediments failed in a brittle manner. Isolated bodies of debris-rich and foliated glacial ice form the contact between the raft of ES Fm and the underlying raft of Bft Fm (Fig. 9d). The ice appears to form broadly tabular rafts that consistently bracket rafts of ES Fm and Bft Fm. Because the glacial ice forms part of the thrust sequence, rather than crosscutting the sequence, it is likely that it was emplaced contemporaneously.

2.2.3. Sub-domain A2

Sub-Domain A2 is located at the very northern end of Domain A where a postglacial gully (Fig. 5) has exposed a section oriented EW (~ 96 m wide and ~ 33 m high) composed of rafts of ES Fm, glaciomarine diamict and Kk Fm that pass distally (coastward) into folded Kk Fm (Fig. 10a). The most proximal (landward) units comprise a low-angle, thrust-faulted raft of ES Fm bracketed by two rafts of Kk Fm (Fig. 10a). The rafts of ES Fm and Kk Fm dip at 10° orientated towards 120° , a direction that is consistent with the widespread southeast direction of thrust-faulted rafts throughout Domain A. This style of deformation presumably records a dominant compressional stress field generated by ice advancing from the source basin. Three imbricately stacked rafts of glaciomarine diamict, Kk Fm, and ES Fm truncate the low-angle, thrust-faulted rafts (Fig. 10b). The stacked rafts have been rotated into near vertical positions with dips of 75° - 85° orientated towards 280° . The high dip of the stacked rafts inclined away from the source basin, suggests that they have been back thrust into position, most likely in response to sustained lateral compaction and the buildup of back stress. Bracketing all the rafts in this proximal zone are intensely brecciated *mélange* zones displaying rip-ups that attest to a period of shear deformation (Fig. 7a, e and f). The base of deformation could not be observed due to a lack of exposure and likely extends below the gully bottom to a basal décollement.

The distal part of Sub-Domain A2 comprises Kk Fm displaying large-scale isoclinal folds fronted (coastward) by the core of a recumbent fold (Fig. 6c). The isoclinal folds have been compressed and subsequently thrust-faulted, leaving them rootless, with their original orientations indiscernible. The dissecting thrust-faults dip at $\sim 45^\circ$ orientated towards $\sim 120^\circ$ and were likely formed under the same stress regime as the low-angle, thrust-faulted rafts in the proximal zone of A2. The most distal part of A2 displays the core of a ~ 25 m long and ~ 30 m wide recumbent fold, with a plunge of $\sim 20^\circ$ orientated towards $\sim 350^\circ$. The fold displays no evidence of brittle deformation and records a period of continued ductile deformation by simple shear.

The magnitude and style of deformation changes clearly with distance along Sub-Domain A2, progressing from complex thrust faulted rafts in the proximal zone (brittle deformation), to largescale isoclinal folds dissected by thrust-faults in the central zone (ductile and brittle deformation), to large-scale recumbent folds in the distal zone (ductile deformation). This pattern of deformation, along with the general orientation of thrust-faults (toward the southeast), suggests that the section was initially deformed by a compressional stress regime imparted by an ice sheet advancing from the southeast. The development of intense shear zones and the onset of overfolding indicates that a later deformation event subsequently reformed the section.

2.2.4. Domain B

Domain B forms the central part of the Worth Point section (2.2 km wide) and displays the greatest range of deformation (Fig. 5). This diversity is attributed to the presence of all eight lithofacies and hence their different responses to glacially-imposed stress, and to the strong overprinting of deformation structures generated by multiple intervals of overriding. The southern and central parts of Domain B are characterized by thrust-faulted rafts of Kk Fm displaying convoluted, overturned folds that have a wide range of dip between 10 and 90° but a consistent orientation towards ~100°. These rafts of Kk Fm are intercalated with more localized thrust-faulted rafts of ES Fm that display a similarly wide range of dip between 10 and 90° also orientated towards ~100°. More gently dipping (0-45°) thrust faulted rafts of glaciomarine diamict orientated towards w 130° are also common throughout Domain B. However, the glaciomarine rafts consistently cross-cut the thrust-faulted rafts of Kk Fm and ES Fm, requiring that they were emplaced during a later event. Nonetheless, the Kk Fm, ES Fm and glaciomarine diamict rafts have all been thrust-faulted into position by a compressional stress regime. Both the thrust-faulted rafts of Kk Fm and the cross-cutting thrust-faulted rafts of glaciomarine diamict have been subsequently dissected by dense networks of faults that commonly run perpendicular to southeast-dipping bedding planes and thrust faults.

The nature of faulting within the Kk Fm and glaciomarine diamict is so pervasive that the deformed units should be classified as breccias. Brecciation of the Kk Fm and glaciomarine diamict was likely contemporaneous, recording an even later deformation event. A lack of brecciation in the associated rafts of thrust-faulted ES Fm probably relates to the coarse-grained and permeable nature of this bedrock, which would have promoted lower porewater pressures and higher shear strengths. Bodies of debris-rich, buried glacial ice (<20 m²) are intercalated with thrust-faulted rafts of Kk Fm and ES Fm, and were presumably emplaced during initial compressional thrust-faulting. The buried glacial ice is not associated with a diamict, and was likely emplaced proglacially. Ground ice also commonly occupies thrust-faults, contacts between different lithologic units, and other easily exploitable spaces within the strata.

The central part of Domain B is capped by glaciofluvial sand and gravel and fragmented pockets of diamict (Fig. 5). The glaciofluvial sand and gravel infill three shallow (<5 m deep) and wide (~40 m wide) channels that incise the uppermost strata, including buried glacial ice. The gravel is coarse, poorly-sorted, and sub-horizontally bedded, with limited evidence for post-depositional deformation. Overlying the glaciofluvial sand and gravel with an angular unconformity are two pockets of consolidated diamict (~10 m wide and ~2 m high). The diamict is indurated and characterized by a sandy-silt matrix, highly angular to sub-angular clasts (RWR = 7%; Fig. 4, Site 1) including rare granites and is interpreted as a subglacial till.

The northern part of Domain B is characterized by a glacioteconite (~20 m thick) comprising sheared rafts of Bft Fm, glaciomarine diamict and Kk Fm (B1). The B1 outcrop exposing the glacioteconite forms the most enigmatic site at Worth Point and is easily identifiable by logs and peat (sourced from the Bft Fm) eroding out of the bluffs (Fig. 11a and c). This thick organic unit was originally assumed to be in situ and proposed as the type section for the preglacial Worth Point Fm

(Vincent, 1982, 1983, 1984, 1989, 1990, 1992; Vincent et al., 1984; Matthews et al., 1986; Barendregt et al., 1998).

2.2.5. Sub-domain B1

Sub-Domain B1 is located at the northern end of Domain B where a coastal section oriented N-S (~27 m high and ~20 m wide) exposes a diverse glaciotectonic sequence (Fig. 11a-c). The section has been dissected by a postglacial valley on its southern edge, which exposes an additional 5m of the section, perpendicular to the coast (Fig. 11c). Here, the section is composed of a sheared and deformed mélange of glaciomarine diamict, Kk Fm and Bft Fm that is interpreted to be a glaciotectonite.

A contiguous raft of Bft Fm forms the base of the section. Ongoing melt-out of ground ice in the overlying strata makes it impossible to determine the precise dip of the raft, but bedding within the raft dips 30° orientated towards 130°. Because the gravel is planar-bedded, this dip is considered to record the displacement of the raft itself. A thrust-faulted raft of glaciomarine diamict, displaying widespread evidence of shear, overlies the Bft Fm and forms the base of a thick glaciotectonite mélange (Fig. 11b). The glaciomarine raft contains isolated pods of Bft Fm that have been attenuated, rotated and sheared (Fig. 11d). Disharmonic anticlines and synclines with smaller-scale parasitic folds within the glaciomarine diamict have been cross-cut by thrust-faults and back thrusts. Clastic dykes infilled with wood fragments, peat, sand, and gravel sourced from the basal raft of Bft Fm have been injected upwards into the glaciomarine diamict and commonly exploit pre-existing shear planes and faults (Fig. 11d). Localized zones of massive Bft Fm sand and gravel within the glaciomarine diamict (sourced from the underlying Bft Fm) attest to the fluidization and remobilization of sediment during shearing. The basal raft of Bft Fm clearly formed an aquifer that expelled groundwater under high porewater pressures into the overlying strata.

Semi-coherent rafts of organic-rich beds sourced from the Bft Fm have been preserved within the overlying glaciotectonite. The lowermost organic raft is the most prominent and comprises water-worn but uncompressed logs and wood (Fig. 11b and c). Two overlying rafts comprise laterally continuous peat mats that extend horizontally for ~20 m (Fig. 11b). Although organics have been sheared from the margins of the rafts and incorporated into the surrounding glaciotectonite, the lateral continuity of the rafts and the excellent preservation of organics within the rafts suggest that they were frozen during original transport and deposition. Although Bft Fm wood has not been observed in situ on southern Banks Island, the lake basins directly behind Worth Point are the most probable source for these organic rafts.

A raft of Kk Fm has been stacked above the uppermost organic raft and incorporated into the glaciotectonite mélange. The glaciotectonic sequence extending upward from the Kk Fm raft comprises sheared pods of glaciomarine diamict and Kk Fm with minor pods of sand and peat sourced from the underlying Bft Fm. The sequence distinctly lacks the widespread faults and clastic dykes observed down-section (Fig. 11d) and instead displays crude subhorizontal banding that becomes increasingly more prominent with distance up-section (Fig. 11e and f). Where evidence of fluid injection is observed, it tends to be in the form of small blow-out structures infilled with coarse sand sourced from localized pods of Bft Fm. These smaller-scale blow-outs likely formed in response to ongoing shear deformation. The conspicuous nature of the sediments eroding from the base of Sub-Domain B1 (i.e. whole logs and peat mats) create the impression of decreasing deformation up-section. At the base, a wide variety of lithologic units outcrop, including coarse sand, gravel and organics. These different lithologic units have varying permeability and shear strength that would have responded differently to applied stress. Consequently, a complex mosaic of ductile deformation (in the fine-grained units) and brittle deformation (in the coarse-grained units) would likely have ensued. The sub-horizontal banding in the glaciotectonite farther up-section attests to high cumulative strain and a probable increase in the magnitude of deformation with elevation. This

pattern of cumulative strain up-section has been proposed to characterize many subglacial shear environments (Banham, 1977; Pedersen, 1989; Hiemstra et al., 2007; Benn and Evans, 2010). The possible existence of 'warm' permafrost (close to its melt point) within a subglacial shear zone, may also explain the development of frozen, competent pods of 'hard-frozen' coarse-grained sediment observed within the weaker matrix of 'plastic-frozen' fine-grained sediment (Waller et al., 2011).

Finally, the glacioteconite is capped by w1 m of fining-upward sequences of pebble-granules, silt, and clay. This sequence is interpreted to record the deposition of mass flow deposits into standing water during deglaciation, when unconsolidated sediment was reworked and locally re-deposited in small ponds and basins. Collectively, Sub-Domain B1 comprises a basal raft of Bft Fm overlain by a thick glacioteconite mélange displaying cumulative strain up-section, which in turn has been capped by mass flow deposits.

2.2.6. Domain C

Domain C forms the northernmost and least deformed part of the Worth Point section (1.8 km, Fig. 5). This domain is characterized by low-angle, thrust-faulted and back thrust rafts of Kk Fm, crosscut by thrust-faulted rafts of glaciomarine diamict. Subsequently, narrow, V-shaped gullies have been incised into these units and then infilled with coarse glaciofluvial sand and gravel. Thrust-faulted and back thrust rafts of Kk Fm both display low dips of 10-30°. However, back-thrusted rafts are orientated towards 130°, as is common throughout Domains A and B, and thrust-faulted rafts are orientated towards 80-100°. Throughout Domain C the southeast-dipping back thrusts have been consistently crosscut by the eastward-dipping thrust-faults, reflecting a subsequent E-W oriented stress field and deformation event. The low dip of both sets of thrusts suggest that Domain C did not experience strong compression or lateral compaction, but rather occupied a zone of unconstrained thrust propagation with reduced stress, presumably distal to the ice margin.

The rafts of Kk Fm display low-amplitude gentle to open overfolds and recumbent folds that are truncated by widely spaced (every >30 m) low-angle faults. Localized shear zones exhibiting brecciation along fault planes become increasingly less common towards the northern part of Domain C. The thrust-faulted rafts of glaciomarine diamict orientated towards ~80°, cross-cut the back thrust rafts of Kk Fm dipping towards 130°, but appear to be consistently orientated in the same direction as the thrust-faulted rafts of Kk Fm. Nonetheless, the rafts of glaciomarine diamict display distinctly less ductile deformation than the rafts of Kk Fm. Furthermore, the glaciomarine rafts often cap the Kk Fm towards the top of the bluffs and have been thrust as coherent rafts along distinct eastward-dipping thrust-faults in several locations. Clearly the Kk Fm underwent initial ductile deformation followed by back thrusting imposed by a stress regime oriented SE-NW. After the deposition of glaciomarine diamict a second, E-W orientated stress regime was responsible for thrust-faulting the glaciomarine diamict and some rafts of Kk Fm.

Three prominent V-shaped gullies and several smaller ones (see Fig. 12a and b) incise the Kk Fm and glaciomarine diamict. The gullies descend below the base of the bluffs and therefore grade to a former relative sea level below modern. The gullies are moderately deep (<30 m) compared to their width (~100m) and are separated by narrow, angular interfluvial channels of Kk Fm (<10 m). Laterally continuous, sub-horizontally (and occasionally horizontally) bedded glaciofluvial sand and gravel infill the gullies and are in turn unconformably overlain by fragmented pockets of compact diamict and fining-upward sequences of sand, silt and laminated clay. This infill is interpreted to record a subsequent marine transgression and/or an abundant sediment supply, possibly from a nearby ice margin.

2.2.7. Sub-domain C1

Sub-Domain C1 constitutes the northernmost end of Domain C and has a fully exposed section (~29 m high and ~200 m wide) through one of these gullies (Fig. 5). Here, the infilling gravel is mostly sub-rounded with a minor fraction of sub-angular clasts bearing striations and boulders < 40 cm². The clasts are dominantly quartzites sourced from Victoria Island to the east and occasional granites sourced from mainland Canada to the southeast (Fig. 12a and b). The presence of granites, along with the coarse and unfossiliferous nature of the gravel, distinguishes the glaciofluvial gravel from the preglacial Bft Fm. Two samples from separate beds of sand interbedded with the gravel provide OSL burial dates of 247 ± 17 ka and 407 ± 33 ka (Sheffield Centre for International Drylands Research, UK, 2012). This constrains the glaciofluvial aggradation to the Mid-Pleistocene (*sensu lato*), as well as the presumed marine transgression required to facilitate their aggradation. The gravel appears undisturbed across tens of metres (laterally and vertically) making it difficult to determine if the bedding dip of ~15° towards 080° records minor thrusting as coherent rafts or its original depositional slope (i.e. delta foresets prograding offshore). Nonetheless, the dip direction of the gravel is consistent with the orientation of the second set of thrust-faults observed in the Kk Fm as well as to the glaciomarine diamict throughout Domain C. This suggests that the gravel, glaciomarine diamict, and thrust-faulted Kk Fm were deformed by the same glaciotectonic event following glaciofluvial aggradation.

A clast-supported diamict overlies the glaciofluvial sand and gravel with an angular unconformity (Fig. 3h). The diamict has a compacted clay-silt matrix displaying a wide range of clast size and shape. Clasts within the diamict are faceted and striated, and a clast macrofabric displays an east-west orientation with an S1 eigenvalue of 0.746 (Fig. 4, Site 2). Based on its strong fabric, clast forms, and surface striae, the diamict is interpreted as a subglacial traction till. As such, the till provides direct evidence for the overriding of Worth Point by an ice sheet after a Mid-Pleistocene regression and transgression that incised and later infilled the incision of the V shaped gullies followed by at least one deformation event responsible for the folding and back-thrusting of the Kk Fm. Multiple sequences of poorly sorted clasts and granules, fining-upward into sand, silt and laminated clay, overlie the till. The localized nature of the fining-upward sequences likely reflects the remobilization of unconsolidated glacial deposits and their re-deposition into small ponds and basins via mass flows.

2.3. Deformation styles and structures

At Worth Point, permafrost has preserved deformation styles and structures developed in a wide range of lithologic units, providing insights into lithologic-specific responses to glacially imposed stress regimes (Aber, 1985). Coarse-grained units at Worth Point (Bft Fm, ES Fm, glaciofluvial sand and gravel) are characterized by brittle deformation. These lithologic units commonly form discrete bedrock rafts with well preserved internal bedding and depositional structures (e.g. Figs 7a, 9b and c, 10a and b). These coarse-grained sediments possess high shear strength during deformation due to high frozen porewater content, resulting in large-scale brittle failure along discrete planes of weakness. Coarse-grained sediment is expected to undergo brittle failure when grains are firmly cemented by pore ice, which occurs at temperatures of < -0.5°C in sand (Waller et al., 2012). The presence of permafrost at Worth Point would have helped to maintain temperatures below -0.5 °C, thereby promoting continued largescale brittle failure. Where coarse-grained sediment displays minor ductile deformation, it is closely associated with the pervasive deformation of the surrounding sediment, as observed within the glaciotectonite *mélange* at Domain B1 (Fig. 11d). This minor ductile deformation may relate to an increase in glacially-imposed stress and/or an increase in temperature (warming of permafrost) towards the pressure-melting point. If temperatures did increase sufficiently, more porewater would be available to create a partially-frozen slurry of ice, water, and sediment. Clearly, increasing the volume of liquidwater would reduce sediment shear strength (greater dilation) and promote ductile deformation (Twiss and Moores, 1992; Waller et al., 2012).

Fine-grained sediment deformation at Worth Point (Kk Fm and glaciomarine diamict) is characterized by complex, large-scale, pervasive folding (e.g. Fig. 6a and b). Because permafrost is inferred to have existed at Worth Point, at least in patches, fine-grained sediment must have undergone ductile deformation at subzero temperatures. The direct juxtaposition of ductile deformation in fine-grained sediment, and brittle deformation in frozen, coarse grained sediment (clearly displayed in Sub-Domain C1) supports the existence of 'warm permafrost' (Waller et al., 2009). Warm permafrost is characterized by temperatures below, but close to, the melt point that permits relatively high amounts of water to exist within fine-grained sediment, possibly down to -7 °C in very fine-grained clays (Tsytoich, 1975; Waller et al., 2012). The existence of warm permafrost would explain the wide range of brittle and ductile deformation observed within different lithofacies at Worth Point.

No doubt, a wide range of interconnected factors influenced the style of deformation at Worth Point, and not all factors are lithologically-specific. The ratio of liquid to frozen porewater contained in sediment - controlling its shear strength e is a function of grain-size and temperature, but also a function of stress (Waller et al., 2012). These variables would have changed at Worth Point as glaciers advanced and retreated across the permafrost terrain. For example, when ice initially advanced over Worth Point, permafrost likely would have been thick and continuous, promoting brittle deformation. However, as ice persisted at Worth Point, permafrost would have warmed from the bottom-up by geothermal heating (Dyke, 1993), favouring the addition of water as well as more ductile deformation (cf. Mooers, 1990; Waller et al., 2012). Therefore, the variable physical properties of the permafrozen sediment at Worth Point, and their consequent response to changeable glacial stress regimes, would have evolved over the course of multiple phases of glaciotectonism. This evolution would have resulted in the diverse spectrum of juxtaposed deformation described here.

Further insights into the dynamics and style of glaciotectonic deformation at Worth Point can be inferred from the analysis of macroscale structures such as shear zones, clastic dykes, and boudins. Shear zones are extensive, spanning a wide range of scales and a broad range of stratigraphic settings (Fig. 7a-f). Shear zones are defined as 'planar zones of relatively intense deformation' that are characterized by brittle faulting and brecciation (Phillips et al., 2011). Brecciation attests to exceptionally high shear stress common to subglacial environments (McCarroll and Rijdsdijk, 2003). The most complex shear zones have developed between sheared bedrock rafts of different lithologies. In these stratigraphic settings, sediment from the two rafts have been ripped-up, detached, and rotated in an inter-raft *mélange* (Fig. 7a, e and 7f). The edges of the sheared rafts often display pervasive brecciation and/or clast imbrication (Fig. 7d), likely recording deformation under a sustained shear stress within a brittle subglacial shear zone (Van der Wateren, 1995; Eyles and Boyce, 1998). Two thin-section samples of Kk Fm were collected from a brecciated surface displaying slickensides that dip 80° towards 180° (Fig. 13a). Analysis of the thin sections provides additional insight into the nature of microscale deformation at Worth Point and record the presence of two dominant fabrics (Fig. 13b and c). A primary fabric (S1) is crosscut, often at right angles, by a secondary fabric (S2). The secondary fabric displays small-scale faults that have displaced the primary fabric and in some areas completely overprinted the primary fabric with a dense network of foliations. Irregular open fissures are common and often develop where larger foliations intersect.

Clastic dykes result from hydrofracturing and are common within the glaciotectonized sequence at Worth Point (Fig. 8b-d). This association is unsurprising given that: a) glaciotectonic environments are regions of high stresses that overpressurize water, and b) faulting and thrusting associated with glaciotectonic deformation provide escape routes for the overpressurized water and sediment (Rijdsdijk et al., 1999; Le Heron and Etienne, 2005; Piotrowski, 2006; Phillips and Merritt, 2008; van der Meer et al., 2009). At Worth Point, it is also possible that patchy permafrost combined with

impermeable strata such as Kk Fm and glaciomarine diamict - further enhanced hydrofracturing by forming aquicludes that confined water to aquifers. Eventually, the overpressurized water and sediment would have burst-out of these aquifers into surrounding strata, exploiting pre-existing faults and fractures. The pressures generated during the burst-out of overpressurized water and sediment would have been sufficient to liquefy the host sediment, injecting it into the hydrofracture (cf. Le Heron and Etienne, 2005).

At Worth Point, two different types of clastic dykes are differentiated. The first comprises clastic dykes that have been injected along recognizable faults and shear planes (i.e. high strain zones). These dykes often narrow upwards and are infilled with coarse grained sand and gravel sourced from the Bft Fm (Figs. 8a and b). Such characteristics indicate that the dykes formed under high hydraulic pressure released in a single event, leading to the deposition of the coarse sand and gravel as a massive unit. Blocked subaerial escape routes (possibly due to the presence of ice) may have allowed hydraulic pressures to build to high levels, resulting in debris liquefaction and the entrainment of large cobbles within the escaping fluid from host aquifers. The narrowing-upward configuration of the dykes suggests that they were expelled upward into the strata from an underlying aquifer. Similar upward-filled clastic dykes have been described from a subglacially glaciotectionised stratigraphic sequence at Killiney Bay, Ireland (Rijsdijk et al., 1999). There, the host aquifer also comprised permeable coarse gravel that became hydraulically confined by an impermeable unit of overlying till. The resulting clastic dykes are up to 7m long, frequently branch into complex geometries, and yet remain rooted in their source gravel aquifers (Rijsdijk et al., 1999). At Worth Point, the upwardfilled, coarse-grained dykes occasionally crosscut one another (Fig. 8b). Such cross-cutting patterns record multi-phase hydrofracturing within the same water-escape route that follows major shear planes and fault surfaces. Comparable 'high strain zones' at the contact between thrust-faulted rafts are known to have provided a focus for hydrofracturing during subglacial glaciotectionism at Clava, Scotland (Phillips and Merritt, 2008). Similarly, coarse grained clastic dykes at Worth Point likely reflect hydrofracturing in a subglacial setting.

The second type of clastic dyke is closely associated with strata displaying evidence for compressional deformation. These dykes comprise finer branching networks of narrow (<20 cm wide) channels infilled with laminated sand and clay (Fig. 8c). These laminated clastic dykes clearly record hydrofracturing under lower hydraulic pressure that permitted the sorting of grain size during settling and infilling (van der Meer et al., 2009). These dykes are commonly injected along smaller faults and joints (mostly in the Kk Fm) and are often truncated by faults themselves. This second type of clastic dyke is considered to have developed in an ice-marginal setting when compressional stresses overpressurized aquifers, but the potential for fluid to escape to the surface, unimpeded by ice, resulted in lower hydraulic pressure. Boudins are widespread deformation structures throughout Domain A. Here, they are composed of coarse-grained Bft Fm sand and gravel, and form streamlined inclusions within complexly deformed Kk Fm (Fig. 6d). The boudins consistently display attenuation in a sub-horizontal direction and have been transported within a plastic Kk Fm matrix. These orientated boudins support deformation within a ductile shear zone.

3. Interpretation

The internal architecture of Worth Point accords with the surficial geomorphology comprising an ice-thrust hill <50 m asl that steepens distally (coastward, Fig. 2). Subtle crescentic ridges forming the crest of the hill are assumed to reflect the position of prominent thrust rafts outcropping beneath the capping unit of subglacial till. Two lakes with a similar orientation to the hill are located directly inland and are interpreted to occupy the source depression from which the hill was derived (Fig. 2). Consequently, the landform is interpreted as a hill-hole pair and similar examples commonly flank the west coast of Banks Island farther north. Construction of the Worth Point hill-hole pair is attributed to the advance and overriding of southwest Banks Island by thin, cold based ice margins

emanating from divides to the southeast during the Mid-Pleistocene (*sensu lato*) and Late Wisconsinan (Lakeman and England, 2013). Geomorphic evidence, primarily the configuration of deglacial ice-marginal meltwater channels, indicates that Laurentide ice crossed the interior of Banks Island during the Late Wisconsinan, including the Kellett and Lennie River valleys surrounding Worth Point (Fig. 2; Vaughan and England, in prep). Of these, ice descending the Kellett River Valley, south of Worth Point, is considered the primary source for constructing the Worth Point hill-hole pair. Nonetheless, convergence of cold-based ice lobes from both the Kellett and Lennie River valleys likely contributed to multiple periods of glaciotectonism along the intervening coastline (Fig. 2).

Although bathymetric profiles support westward ice flow through Amundsen Gulf (Blasco et al., 2005; MacLean et al., 2012), the passage of this trunk ice onto Banks Island appears to have been limited to a prominent lateral moraine paralleling its south coast (<1 km inland). Therefore, trunk ice in Amundsen Gulf is not invoked to explain glaciotectonism at Worth Point. Permafrost at Worth Point, and along the west coast of Banks Island, undoubtedly augmented glaciotectonism. Although current permafrost on southwest Banks Island is continuous and likely >750 m thick (Taylor et al., 1996), periods of permafrost degradation likely occurred in the past. For example, Worth Point is located on the Beaufort Sea coast where raised marine sediments OSL dated between 94 ± 4.2 ka and 118 ± 5.7 ka (Lakeman and England, 2013; Vaughan et al., in prep.) support a Sangamonian (*sensu lato*) marine transgression that would have degraded terrestrial permafrost thickness below ~ 11 m asl today. Earlier marine transgressions (to unspecified elevations) are also inferred at Worth Point based on the deposition of glaciomarine diamicts observed in Domains B and C, as well as the glaciofluvial aggradation observed in Domain C. The occurrence of thinner permafrost would have facilitated thrusting and deformation at Worth Point, like thrust-dominated landforms noted elsewhere throughout the Canadian High Arctic (Evans and England, 1991). In these cases, thrust-block moraines produced by late Holocene readvances are widespread on valley floors well below marine limit. Here, the reaggradation of permafrost is shallow (10's vs 100's of metres) due to the recent emergence of areas below w 40 m asl that favour surface décollement produced by widespread Neoglacial readvances (Evans and England, 1991). A similar relationship between degraded (thinner) permafrost and ice-thrusting would have characterized Worth Point following earlier marine transgressions/ regressions associated with ice advance and retreat. The close association between thrust-dominated landforms, such as thrust block moraines and hill-hole pairs, and former areas of shallow modern permafrost at low elevations in the Canadian Arctic raises the likelihood that shallow permafrost is a primary condition for the initiation of thrusting (Evans and England, 1991; Boulton, 1999). A critical range of permafrost and glacier ice thicknesses may exist, within which deformation is promoted by effective ice-bed coupling, provided that suitable material for deformation is also present. Alternatively, others have proposed that glaciotectonic deformation and thrust mass construction is due to glacier surging (Sharp, 1985, 1988; Croot, 1988; Evans and Rea, 1999, 2003; Evans et al., 2007). If so, former ice sheet surges may have been involved in the production of some Banks Island moraines regardless of accompanying permafrost characteristics (cf. Evans et al., 1999, 2008). Currently, the formation of the Worth Point hill-hole pair is attributed to thin, cold-based ice lobes that would have been unlikely to surge.

A bedrock boundary approximately 2 km east of Worth Point may have contributed to glaciotectonism because the source depression of the hill-hole pair coincides with the contact between Kk Fm to the west (coast) and Bft Fm to the east (inland). The coarse Bft Fm is permeable, and therefore during ice advance, expelled groundwater could drain freely through/beneath it towards the impermeable Kk Fm. Hence, when ice reached the fine-grained Kk Fm, increased groundwater drainage there would have raised porewater pressures and reduced its frictional strength, serving to initiate glaciotectonic deformation coastward of this bedrock boundary. Furthermore, permafrost is inferred to have played a fundamental role in influencing the subsequent style of deformation at Worth Point. For example, it is thought that permafrost was

locally warm and patchy, promoting hydrofracturing along with the development of contrasting deformation styles in coarse-grained (brittle) and fine-grained (ductile) lithofacies. Such permafrost characteristics have been inferred to explain similarly contrasting deformation observed in glaciotectionized stratigraphic sequences in the Mackenzie Delta to the south of Banks Island (Waller et al., 2012). As well, the wide range of lithologic units in the subsurface at Worth Point may have further enhanced deformation (Boulton, 1972). Contacts between lithologic units appear to have formed décollement planes along which displacement occurred more readily, promoting the formation of discrete bedrock rafts. Moreover, because the style and magnitude of deformation is directly related to the grain size, sorting, and cohesion of sediments, the wide range of lithofacies at Worth Point would have produced a range of deformation processes and structures. This diversity of structures was enhanced further by the strong overprinting and cross-cutting of multiple generations of deformation structures and styles throughout Domains A-C. Based on this overprinting, two distinct glaciotectonic events with multiple stress regimes have been identified. Key stratigraphic evidence to support each glaciotectonic event is presented below.

3.1. Relative chronology of glaciotectonism and relative sea level change

3.1.1. Glaciotectonic event 1

Throughout the Worth Point stratigraphic sequence (Domains A-C), the dominant orientation of thrust-faulted rafts is SE-NW. Therefore, it is assumed that the ice margin responsible for this deformation also advanced from the southeast, down the Kellett River (Fig. 2). The location of lakes and tundra ponds in a basin ~2 km to the southeast of the bluffs reinforces the interpretation that they mark the source depression from which the ice-pushed hill at Worth Point originated. If so, the bluffs provide an exposure at a right-angle to the thrust, with Domains A-C displaying a progressive proximal to distal deformation sequence (Fig 14, Box 8). All Domains are dominated by thrust-faulting produced by compression, most likely generated ice-marginally, as manifested today across the northern part of the CAA (Evans and England, 1991; McCarroll and Rijdsdijk, 2003). The dip and number of thrust-faulted rafts decrease northward (from Domain A-C) because the compression from the former ice margin also decreases in this direction (cf. Mulugeta and Koyi, 1987).

Accordingly, the most proximal area (Domain A) displays imbricately stacked rafts of thrust-faulted bedrock (nearly vertical). Towards the surface, these bedrock rafts have been truncated by more gently dipping back thrust rafts. This back thrusting is well displayed in Sub-Domain A2 (Fig. 10b) where back-thrust rafts of ES Fm, Kk Fm and glaciomarine diamict truncate thrust-faulted bedrock. As the dip of thrust-faulted bedrock rafts decreases northward in Domain B, fold preservation increases. Large-scale isoclinal folds with drag structures are widespread in Domain B, and likely evolved from open, symmetric folds that steepened and overturned in places, becoming unrooted during lateral compression. Domain C is the most distal and least deformed domain, displaying large, open, symmetric folds truncated by low angle thrust-faults and back thrusts. This pattern of thrust-faulting, back thrusting, and stacking in proximal, intermediate, and distal positions is typical of what is described as ice-marginal piggy-back thrusting (Rotniki, 1976). Piggy-back thrusting involves the development of new thrusts distal to previously active thrusts, resulting in the stacking of proximal thrusts into increasingly steeper positions (as displayed in Domain A). This includes the transport of these proximal thrusts, piggy-back style, onto less steeply dipping, distal thrusts below (as displayed in Domain C and modelled by Mulugeta and Koyi, 1987). In contrast, back thrusts result from the build-up of back stress during the later stages of stacking and lateral compaction. The overall pattern of progressively more ductile deformation with distance from the ice margin (toward Domain C) is presumably related to an increased preservation of folds in the distal zone where fewer, lower-angle thrusts truncate the previously folded strata. Comparable proximal to distal glaciotectonic sequences are common at former ice-margins, including the Rubjerg Knude glaciotectonic complex in northern Denmark (e.g. Pedersen, 2005), and the polydeformed Quaternary stratigraphy of East Anglia, England (e.g. Phillips et al., 2008).

Throughout Domains A-C narrow, branching networks of clastic dykes infilled with laminated sand and clay are closely associated with deformation structures generated by ice-marginal thrusting. This stratigraphy is consistent with this setting, where over pressurized water would have been expelled preferentially along pre-existing faults, joints, and lithologic contacts toward the unconfined surface beyond ice. The movement of pressurized fluid along these planes of weakness would have reduced the frictional strength of the adjacent sediment, promoting displacement and thrust propagation. Blocks of buried glacial ice containing far travelled erratics from the Precambrian Shield on the Canadian mainland also form part of the thrust sequence, and would have been thrust into position contemporaneously. It is simplest to envisage this glacial ice pre-existing at Worth Point prior to glaciotectonic event 1, rather than being sourced from the ice sheet responsible for glaciotectonic event 1 itself. Because the glaciotectonite (Domain B), glaciomarine diamict, glaciofluvial sand and gravel, and subglacial till (Domains B and C) do not form part of the piggy-back sequence, they were presumably deposited and deformed after initial ice-marginal compression.

Throughout Domains AeC, a second generation of deformation structures is imprinted onto the thrust sequence. The overprinted structures are characterized by simple shear, characteristic of subglacial deformation (McCarroll and Rijdsdijk, 2003). Domain B best preserves sediments and deformation structures generated by this later event, including a w20 m thick glaciotectonite mélange, intensely brecciated bedrock, and widespread macroscale shear structures such as boudins (e.g. Fig. 11def). Thin section analysis of brecciated Kk Fm sampled from Domain B indicates that this deformation was penetrative, with sediment modification at the granular scale (Fig. 13b and c). This reflects deformation within faulted rafts rather than displacement along fault planes. Subhorizontal strain banding and intense ductile deformation within the glaciotectonite mélange (Domain B1) provide further support for high cumulative strains, probably within a ductile subglacial shear zone (McCarroll and Rijdsdijk, 2003). Collectively, this deformation records the development of a subglacial shear zone when a later ice advance overrode Worth Point.

The southeast orientation of shear planes and shear-related foliation (mostly in Domain B) associated with subglacial shear are consistent with the southeast orientation of thrust-faulted rafts developed during previous ice-marginal compression (throughout Domains A-C). The simplest interpretation of the uniform orientation of the deformed strata during both ice-marginal and subglacial deformation is that they relate to the same stress field from the same ice sheet advancing from the southeast, possibly oscillatory in nature. Subglacial deformation resulted in the development of recumbent and overturned folds superimposed on the pre-existing structures, creating complex fold interference and boudinage (Fig. 6a-d). Large clastic dykes are also widely associated with the sheared deformation sequence throughout Domains A-C (Fig. 8b and c), recording hydrofracturing in a subglacial environment.

Two marine transgressions and regressions are recorded in the sequence associated with glaciotectonic event 1. Glaciomarine diamict forms part of the sheared deformation sequence in Domains B and C and is a key component of the glaciotectonite at Sub-Domain B1, but is not observed within the piggy-back thrust sequence. The incorporation of glaciomarine diamict into the sheared sequence indicates that a marine transgression occurred during initial ice-marginal deformation and ice loading, prior to ensuing overriding and subglacial reworking. A following marine regression to below modern sea level is recorded by the incision of glaciofluvial gullies into the compressed and sheared strata. A second marine transgression would explain the aggradation of glaciofluvial sand and gravel infilling the gullies to ~30 m asl. OSL dating of two sand samples associated with the aggradation of the glaciofluvial sand and gravel provide minimum burial dates of 247 ± 17 ka and 407 ± 33 ka (Sheffield Centre for International Drylands Research, UK, 2012), constraining aggradation to the Mid- Pleistocene (*sensu lato*). Consequently, glaciotectonic event 1 must be broadly penecontemporaneous with and/or older than glaciofluvial aggradation, and

glaciotectonic event 2 must be broadly penecontemporaneous and/or younger. A second marine regression following glaciofluvial aggradation is required to account for modern sea level that is currently ~30 m below the top of the infilled gullies.

3.1.2. Glaciotectonic event 2

A final and subtle set of deformation structures characterized by compressional deformation orientated to the east is superimposed on the preceding compressional and shear deformation structures orientated to the southeast. This final deformation is best observed in Domain C, where ice-marginally compressed and subglacially sheared strata (orientated to the southeast) are consistently crosscut by low-angle, thrust-faulted glaciofluvial sand and gravel, Kk Fm, and glaciomarine diamict (orientated to the east). The thrust faulted glaciofluvial sand and gravel preserve what was originally sub-horizontal bedding, suggesting that they were thrust as frozen rafts. A clast macrofabric measured within the overlying till is orientated east-west providing further evidence for an ice advance from the east, overriding Worth Point. The lack of shear in the eastward-dipping sequence suggests that glaciotectonic disturbance was initiated predominantly proglacially.

A significant interval of non-deformation is inferred to have separated glaciotectonic events 1 and 2 based on the time required to incise and infill the glaciofluvial gullies that are OSL dated to the Mid-Pleistocene (*sensu lato*, Domain C). Also, modified permafrost characteristics may have influenced the change to dominantly brittle deformation during glaciotectonic event 2. For example, if permafrost had thickened (i.e. refreezing patches) and/or become colder (i.e. inhibiting the existence of water) prior to glaciotectonic event 2, then the strata would have been more susceptible to brittle failure.

3.2. Glaciotectonic model

Collectively, two glaciotectonic events and two marine transgressions and regressions have been reconstructed from the polydeformed Worth Point section (Fig. 14). These are summarized below:

2) Glaciotectonism by a Mid-Pleistocene ice sheet. Initial ice sheet advance from the southeast produced a hill-hole pair and deformed the strata ice-marginally under compression, creating a distinct proximal to distal thrust sequence (Fig.14, Boxes,1-2). A marine transgression, facilitated by glacial loading, reworked the deformed strata and deposited a glaciomarine diamict (Fig. 14, Boxes 3-4). A readvance or ongoing advance of the ice sheet then overrode and reformed the strata, imprinting shear deformation structures and depositing a thick glacioteconite *mélange*, likely in a subglacial shear zone (Fig. 14, Boxes 4-5). As ice retreated from Worth Point, initial emergence resulted in a regression to below modern sea level, allowing incision of outwash gullies into Domain C. Subsequent submergence led to the aggradation of glaciofluvial sand and gravel in these gullies (Fig. 14, Box 6), which entrapped sediments until the ice sheet retreated beyond the regional drainage divide 30 km inland occasioning renewed emergence. No subsequent drainage has re-excavated these gullies but rather it has remained confined to the Lennie and Kellett river valleys. The OSL burial dating of glaciofluvial sand to 247 ± 17 ka or alternatively 407 ± 33 ka supports an extensive ice sheet crossing Banks Island during the Mid-Pleistocene (*sensu lato*).

2) Glaciotectonism by the Laurentide Ice Sheet (LIS). During the Late Wisconsinan the LIS is recognized to have overridden north and central Banks Island (England et al., 2009; Lakeman and England, 2012) as well as Worth Point (Vaughan and England, in prep). This advance is the most likely candidate for redefining the strata proglacially and depositing a capping till (glaciotectonic event 2, Fig. 14, Box 7). Absolute age-dating is provided by OSL analyses, whereas the relative timing of glaciotectonic events is derived from crosscutting relationships and superimposed deformation styles. Based on these relationships, deformation by an oscillatory Mid-Pleistocene ice sheet

(ancestral LIS) followed by the Late Wisconsinan LIS is the simplest explanation of the glaciotectonic sequence at Worth Point.

4. Discussion and conclusions

The evolution of the polydeformed stratigraphic sequence at Worth Point has implications for: a) characterizing process-form relationships of hill-hole pairs; b) understanding the nature of deformation in diverse permafrozen lithologic units imposed by glacial stress; c) constraining regional glacial and sea level histories, and; c) testing the validity of a formerly-proposed environmental framework of Banks Island extending back to the Early Pleistocene (Vincent, 1982, 1983, 1984, 1990; Barendregt et al., 1998). The mechanisms that govern the formation of hill-hole pairs in permafrost terrain remain uncertain (Aber and Ber, 2007). High porewater pressures generated in the proglacial foreland by glacier surging have been proposed for the establishment of hill-hole pairs in Scotland (Evans and Wilson, 2006), and glaciotectonic deformation in Iceland, Svalbard, and the Canadian High Arctic (e.g. Kalin, 1971; Croot, 1988; Copland et al., 2003). At Worth Point, the role of past ice-marginal surging is difficult to constrain; however, the thin lobes of ice invoked for the valleys of western Banks Island seem more suited for cold-based ice glaciologically and climatologically.

Consequently, the operation/interplay of other factors are inferred to facilitate hill-hole construction at Worth Point, including: a) high porewater pressures developed in taliks occupying otherwise impermeable and permafrozen sediment (Kk Fm) like the modern Mackenzie Delta (Mackay, 1959, 1989); b) a basal décollement plane (shallow permafrost) above which deformation is initiated as characterized adjacent to modern glaciers that have advanced into recently emergent valleys of the Canadian High Arctic (Evans and England, 1991); c) effective ice-bed coupling between cold-based ice and permafrost terrain (Matthews and Mackay, 1960; Mackay and Matthews, 1964; Waller et al., 2012); and d) diverse lithologic units that permit effective transmission of stress by failure along unit contacts (décollement planes; Benn and Evans, 2010). At a regional scale, the spatial distribution of hill-hole pairs across Banks Island can help to elucidate the primary factors controlling glaciotectonism. Here, hill-hole pairs are clustered in a belt ~200 km long and <20 km wide flanking the island's west coast. The former extent of this belt is unknown because ongoing coastal erosion (submergence) throughout most or all of the Holocene has removed an unidentifiable volume of sediment. Nonetheless, glaciotectonized strata on Robillard and Phillips island (~10 km off the northwest coast of Banks Island) suggest that glaciotectonic disturbance extended at least this far offshore (T. Lakeman, pers comm. 2010). The hill-hole belt broadly coincides with the margin of outcropping Kk Fm and may also coincide with the zone of former marine submergence that would have occasioned permafrost degradation. Therefore, the development of high porewater pressures in impermeable sediment (Kk Fm) and the existence of a basal décollement surface (thinner permafrost) are proposed to have been the primary factors governing hill-hole construction on Banks Island. The influence of these process-form relationships in other permafrost terrains requires further investigation.

Initial construction of the Worth Point hill-hole pair is constrained to the Mid-Pleistocene (*sensu lato*), and as such constitutes the oldest hill-hole pair currently reported in Canada. Herschel Island, offshore from the Yukon Coastal Plain, constitutes another large-scale hill-hole pair that was formed during the last glacial maximum (LGM) on the exposed (emergent) Beaufort Sea Shelf where thin permafrost likely aggraded in the path of the advancing northwest LIS (Mackay, 1959; Fritz et al., 2012). Herschel Island is the largest ice-pushed hill currently recognized in the Canadian Arctic and locally demarcates the maximum extent of the northwest LIS adjacent to mainland Canada. Elsewhere on western Banks Island, a similar Late Wisconsinan age for the hill-hole belt is supported by MIS 3 ice transported shells lying distal to it, and by meltwater channels associated with the hill-hole pairs that grade to Late Wisconsinan marine limit (Lakeman and England, 2013; Vaughan and

England, in prep). This Late Wisconsinan signature may be superimposed over the Mid-Pleistocene record with the assumption that other hill-hole pairs across Banks Island are polydeformed, as exemplified at Worth Point. The investigation and absolute dating of additional stratigraphic sequences across west Banks Island is required to address and clarify the long-term evolution of its glaciotectionic landforms and sediments. The deformation of lithologically-variable permafrozen sediment in ice-marginal and subglacial environments remains poorly understood (Waller et al., 2012). This is because the most investigated glaciotectionized stratigraphic sequences are located in mid-latitudes, where their original structures have been disturbed or lost as ice cores (initially permafrost) degraded (Dyke and Savelle, 2000). Worth Point provides an exceptional opportunity to document and understand the deformation of permafrozen sediments because: a) permafrost likely has existed continuously on Banks Island since the Mid-Pleistocene or earlier, permitting exceptional preservation of detailed deformation structures and styles imparted during multiple episodes of glaciotectionism; b) a wide range of lithologic units are present at Worth Point, providing diverse opportunities to observe lithologically-specific responses (from brittle to ductile) to glacially-imposed stress (from compression to shear).

At Worth Point, ground ice and debris-rich glacial ice dating to the Mid-Pleistocene (*sensu lato*) or earlier (emplaced during or prior to glaciotectionic event 1) have been preserved for at least two intervening glacial-interglacial cycles, persisting through multiple glaciotectionic events. The preservation of buried glacial ice and ground ice in permafrost is a common and well-documented phenomenon throughout the western Canadian Arctic (e.g. Mackay, 1959; Mackay et al., 1972; O Cofaigh et al., 2003; Murton et al., 2004; Harris and Murton, 2005; Fritz et al., 2012). Early investigations of these buried ice bodies in the western Canadian Arctic inferred them to be *in situ* (epigenetic permafrost) and formed by ice segregation or ice injection (Mackay, 1971, 1989).

However, a growing consensus now recognizes that much of the buried ice became detached from former ice sheets and was then buried and incorporated into the permafrost. This phenomenon has been observed on Banks Island (French and Harry, 1988; Lakeman and England, 2013), Victoria Island (Lorrain and Demeur, 1985; Dyke and Savelle, 2000), the Canadian Arctic mainland (e.g. Mackay et al., 1972; French and Harry, 1990; Murton, 2005), Russian Arctic (e.g. Astakhov and Isayeva, 1988; Svendsen et al., 2004), Svalbard (e.g. Brandt et al., 2007) and Antarctica (e.g. Sugden et al., 1995; Marchant et al., 2002). Furthermore, reported buried ice preserved in permafrost can be ancient. For example, buried glacial ice reported from the southern Kara Sea coast of Russia and from Bylot Island in the CAA is thought to date from the Mid-Pleistocene (Ingolfsson and Lokrantz, 2003; Fortier et al., 2009), whereas buried glacial ice reported from southern Victoria Land in Antarctica is thought to date from the Miocene (Marchant et al., 2002). In unglaciated terrain, ice-rich permafrost >700 ka has also been reported from the Yukon (Froese et al., 2008). The preservation of buried glacial ice tentatively dated to the Mid-Pleistocene or earlier at Worth Point accords with widespread evidence that ancient glacial ice can survive multiple glacial and interglacial cycles when incorporated into permafrost, and also serves to highlight the antiquity of permafrost in the CAA. Such thermal inertia exhibited by permafrost on Banks Island has important implications for our understanding of modern climate change (IPCC AR5, 2013), especially if this long-established buried ice begins to degrade.

The revised glaciotectionic model for Worth Point reported here replaces the purportedly *in situ*, horizontally-bedded stratigraphic sequence that formed an elaborate, long-standing and widely cited environmental framework for the western CAA, spanning the Neogene and Quaternary (Vincent, 1982, 1983, 1984, 1989, 1990, 1992; Vincent et al., 1984; Matthews et al., 1986; Barendregt et al., 1998). The current reinterpretation of glaciations and glacioisostatically forced marine transgressions and regressions at Worth Point help to constrain the extent and style of glaciation along the polar continental shelf of the Arctic Ocean where increasing interest is being

placed on the age and origin of deep scouring of the circumpolar seafloor (Polyak et al., 2001; Jakobsson et al. 2008, 2010, in press). This record from the westernmost CAA also contributes to an improved understanding of the relationship between the northwest margin of the LIS and the adjoining Ice Age refugium of Beringia that had incorrectly included Banks Island during the LGM (England et al., 2009).

Acknowledgements

Primary funding for this research was provided by an NSERC Northern Research Chair and NSERC Discovery Grants to J. England, and Circumpolar/Boreal Alberta Research Grants awarded to J. Vaughan by the Canadian Circumpolar Institute, University of Alberta. Logistical support was provided throughout by the Polar Continental Shelf Program (PCSP, Natural Resources Canada). E. Moss, C. Lafarge, K. Wolki, and K. Williams provided valued support in the field. T. Lakeman, R. Coulthard, M. Furze, and C. Nixon provided constructive and appreciated insights. Formal reviews by R. Waller and A. S Dyke are acknowledged for their comments that additionally improved the paper.

References

- Aber, J.S., 1985. The nature of glaciotectonism. *Geol. Mijnb.* 64, 389-395.
- Astakhov, V.I., Isayeva, L.L., 1988. The 'Ice Hill'; an example of 'retarded deglaciation' in Siberia. *Quat. Sci. Rev.* 7, 29-40.
- Aber, J.S., Ber, A., 2007. *Glaciotectonism. Developments in Quaternary Science* 6. Elsevier, Amsterdam.
- Banham, P.H., 1977. Glacitectorites in till stratigraphy. *Boreas* 6, 101-105.
- Barendregt, R.W., Vincent, J.-S., Irving, E., Baker, J., 1998. Magnetostratigraphy of Quaternary and late tertiary sediments on Banks island, Canadian arctic archipelago. *Can. J. Earth Sci.* 35, 147-161.
- Benn, D.I., Evans, D.J.A., 2010. *Glaciers and Glaciation*, second ed. Hodder Education, London.
- Blasco, S., Bartlett, J., Bennett, R., Hughes-Clark, J., Maclean, B., Scott, S., Sonnichsen, G., 2005. Northwest passage marine sediments: a record of Quaternary history and climate change. Arctic Workshop abstract, March 9th-12th. University of Alberta, Edmonton, Canada.
- Boulton, G.S., 1999. The sedimentary and structural evolution of a recent push moraine complex: Holstrombreen, Spitsbergen. *Quat. Sci. Rev.* 18, 339-371.
- Brandt, O., Langley, K., Kohler, J., Hamran, S.-E., 2007. Detection of buried ice and sediment layers in permafrost using multi-frequency Ground Penetrating Radar: a case examination on Svalbard. *Remote Sens. Environ.* 111, 212-217.
- Clark, D.L., Vincent, J.-S., Jones, G.A., Morris, W.A., 1984. Correlation of marine and continental glacial and interglacial events, Arctic Ocean and Banks Island. *Nature* 311, 147-149.
- Copland, L., Sharp, M.J., Dowdeswell, J.A., 2003. The distribution and flow characteristics of surge-type glaciers in the Canadian High Arctic. *Ann. Glaciol.* 36, 73-81.
- Craig, B.J., Fyles, J.G., 1960. Pleistocene Geology of Arctic Canada. Geological Survey of Canada. Paper 60-10, 21.
- Croot, D.G., 1988. Glaciotectonics and surging glaciers: a correlation based on Vestpitsbergen, Svalbard, Norway. In: Croot, D.G. (Ed.), *Glaciotectonics: Forms and Processes*. Balkema, Rotterdam, pp. 33-47.
- Darby, D.,A., 2003. Sources of sediment found in sea ice from the western Arctic Ocean, new insights into processes of entrainment and drift patterns. *J. Geophys. Res. Oceans* 108, 13.1-13.8.
- Dyke, A.S., 1993. Landscapes of cold-centred Late Wisconsinan ice caps, Arctic Canada. *Prog. Phys. Geogr.* 17, 223-247.
- Dyke, A.S., Savelle, J.M., 2000. Major end moraines of Younger Dryas age on Wollaston Peninsula, Victoria Island, Canadian Arctic: implications for paleoclimate and for formation of hummocky moraines. *Can. J. Earth Sci.* 37, 601-619.
- Ehlers, J., Gibbard, P.L. (Eds.), 2004. *Quaternary Glaciations: Extent and Chronology. Part II: North America. Developments in Quaternary Science*, vol. 2. Elsevier, Amsterdam.

- Ehlers, J., Gibbard, P.L., Hughes, P.D. (Eds.), 2011. *Quaternary Glaciations: Extent and Chronology: a Closer Look*. Elsevier, Amsterdam.
- England, J.H., Furze, M.F.A., Doupe, J.P., 2009. Revision of the NW Laurentide Ice Sheet: implications for paleoclimate, the northeast extremity of Beringia, and Arctic Ocean Sedimentation. *Quat. Sci. Rev.* 28, 1573-1596.
- Evans, D.J.A., England, J.H., 1991. Canadian landform examples 19: high Arctic thrust block moraines. *Can. Geogr.* 35, 93-97.
- Evans, D.J.A., Rea, B.R., 1999. Geomorphology and sedimentology of surging glaciers: a landsystems approach. *Ann. Glaciol.* 28, 75-82.
- Evans, D.J.A., Salt, K., Allen, C.S., 1999. Glacitected lake sediments, Barrier lake, Kanninaskis Country, Canadian Rocky Mountains. *Can. J. Earth Sci.* 36, 395-407.
- Evans, D.J.A., Rea, B.R., 2003. Surging glacier landsystem. In: Evans, D.J.A. (Ed.), *Glacial Landsystems*. Arnold, London, pp. 259-288.
- Evans, D.J.A., Wilson, S.B., 2006. Scottish landform example 39: the lake of Menteith glacial hill-hole pair. *Scott. Geogr. J.* 122, 352-364.
- Evans, D.J.A., Twigg, D.R., Rea, B.R., Shand, M., 2007. Surficial geology and geomorphology of the Brúarjökull surging glacier landsystem. *J. Maps*, 349-367.
- Evans, D.J.A., Clark, C.D., Rea, B.R., 2008. Landform and sediment imprints of fast glacier flow in the southwest Laurentide Ice Sheet. *J. Quat. Sci.* 23, 249-272.
- Eyles, N., Boyce, J.I., 1998. Kinematic indicators in fault gouge: tectonic analog for soft-bedded ice sheets. *Sediment. Geol.* 116, 1-12.
- Fortier, F., Godin, E., Kanevskiy, M.Z., Allard, M., 2009. Middle Pleistocene (?) buried glacial ice on Bylot Island, Canadian Arctic Archipelago. *EOS Trans. Am. Geophys. Union* 90, 52.
- Fritz, M., Wetterich, S., Schirrmeister, L., Meyer, H., Lantuit, H., Preusser, F., Pollard, W.H., 2012. Eastern Beringia and beyond: Late Wisconsinan and Holocene landscape dynamics along the Yukon coastal Plain, Canada. *Palaeogeogr. Palaeoclimatol. Palaeoecol.* 319, 28-45.
- French, H.M., Harry, D.G., 1988. Nature and origin of ground ice, Sandhills moraine, southwest Banks island, western Canadian arctic. *J. Quat. Sci.* 3, 19-30.
- French, H.M., Harry, D.G., 1990. Observations on buried glacier ice and massive segregated ice. Western Arctic Coast, Canada. *Permafrost Periglacial Process.* 1, 31-43.
- Froese, D.G., Westgate, J.A., Reyes, A.V., Enkin, R.J., Preece, S.J., 2008. Ancient permafrost and a future, warmer arctic. *Science* 321, 1648.
- Fyles, J.G., Hills, L.V., Matthews, J.V., Barendregt, R., Baker, J., Irving, E., Jette, H., 1994. Ballast Brook and Beaufort formations (Late Tertiary) on northern Banks island, arctic Canada. *Quat. Int.* 22-23, 141-171.
- Harris, C., Murton, J.B., 2005. *Interactions between Glaciers and Permafrost: an Introduction*, vol. 242. Geological Society, London, pp. 1-9.
- Hiemstra, J.F., Evans, D.J.A., O'Coiffaigh, C., 2007. The role of glacial rafting and comminution in the production of subglacial tills: examples from southwest Ireland and Antarctica. *Boreas* 36, 386-399.
- Ingolfsson, O., Lokrantz, H., 2003. Massive ground ice body of glacial origin at Yugorski Peninsula, arctic Russia. *Permafrost Periglacial Process.* 14, 199-215.
- International Panel on Climate Change (IPCC) Co-Chairs of Working Group 1, 2013. Working Group 1 Contribution to the IPCC Fifth Assessment Report Climate Change 2013: the Physical Science Basis. In: Chapter 4: Observations: Cryosphere - Final Draft Underlying Scientific-technical Assessment.
- Jakobsson, M., Polyak, L., Edwards, M.H., Klemen, J., Coakley, B.J., 2008. Glacial geomorphology of the central Arctic Ocean: Chukchi Borderland and the Lomonosov Ridge. *Earth Surf. Process. Landf.* 33, 526-545.
- Kalin, M., 1971. The active push moraine of the Thompson glacier. Montreal McGill University, Axel Heiberg island research. *Rep. Glaciol.* 4, 68.

- Lakeman, T.R., England, J.H., 2012. Paleoglaciological insights from the age and morphology of the Jesse moraine belt, western Canadian Arctic. *Quat. Sci. Rev.* 47, 82-100.
- Lakeman, T.R., England, J.H., 2013. Late Wisconsinan glaciation and postglacial relative sea level change on western Banks Island, Canadian Arctic Archipelago. *Quat. Res.* 80, 99-112.
- Le Heron, D.P., Etienne, J.L., 2005. A complex subglacial clastic dyke swarm, Solheimajökull, southern Iceland. *Sediment. Geol.* 181, 25-37.
- Lorrain, R.D., Demeur, P., 1985. Isotopic evidence for relic Pleistocene glacier ice on Victoria Island, Canadian Arctic Archipelago. *Arctic Alpine Res.* 17, 89-98.
- Mackay, J.R., 1959. Glacier ice-thrust features of the Yukon Coast. *Geogr. Bull. Can.* 13, 5-21.
- Mackay, J.R., 1971. The origin of massive icy beds in permafrost, western Arctic Coast, Canada. *Can. J. Earth Sci.* 8, 397-422.
- Mackay, J.R., Rampton, V.N., Fyles, J.G., 1972. Relic Pleistocene permafrost, Western Arctic, Canada. *Science* 176, 1321-1323.
- Mackay, J.R., 1989. Massive Ice: Some Field Criteria for the Identification of Ice Types. Paper 89-1G. Geological Survey of Canada, pp. 5-11.
- Mackay, J.R., Matthews, W.H., 1964. The role of permafrost in ice-thrusting. *J. Geol.* 72, 378-380.
- MacLean, B., Blasco, S., Bennett, R., Lakeman, T., Hughes-Clarke, J., Kuus, P., Patton, E., 2012. Marine evidence for a glacial ice stream in Amundsen Gulf, Canadian Arctic Archipelago. In: 42nd Annual Arctic Workshop Abstract, March 7th-9th. University of Colorado, US.
- Marchant, D.R., Lewis, A.R., Phillips, W.M., Moore, E.J., Souchez, R.A., Denton, G.H., Sugden, D.E., Potter, N., Landis, G.P., 2002. Formation of patterned ground and sublimation till over Miocene glacier ice in Beacon Valley, southern Victoria Land, Antarctica. *Geol. Soc. Am. Bull.* 114, 718-730.
- Matthews, J.V., Mott, R.J., Vincent, J.-S., 1986. Preglacial and interglacial environments on Banks Island: pollen and macrofossils from Duck Hawk Bluffs and related sites. *Geogr. phys. Quat.* 3, 279-298.
- Mathews, W.H., Mackay, J.R., 1960. Deformation of soils by glacier ice and the influence of pore pressures and permafrost. *Trans. R. Soc. Can.* 54, 27-36.
- McCarroll, D., Rijdsdijk, K.F., 2003. Deformation styles as a key for interpreting glacial depositional environments. *J. Quat. Sci.* 18, 473-489.
- Miall, A.D., 1976. Sedimentary structures and paleocurrents in a Tertiary deltaic succession, northern Banks Island, Arctic Canada. *Can. J. Earth Sci.* 13, 1422-1432.
- Mooers, H.D., 1990. Ice-marginal thrusting of drift and bedrock: thermal regime, subglacial aquifers, and glacial surges. *Can. J. Earth Sci.* 27, 849-862.
- Mulugeta, G., Koyi, H., 1987. Three-dimensional geometry and kinematics of experimental piggyback thrusting. *Geology* 15, 1052-1056.
- Murton, J.B., 2005. Ground-ice stratigraphy and formation at North Head, Tuktoyaktuk Coastlands, western Arctic Canada: a product of glacier-permafrost interactions. *Permafrost Periglacial Process.* 16, 31-50.
- Murton, J.B., Waller, R.I., Hart, J.K., Whiteman, C.A., Pollard, W.H., Clark, I.D., 2004. Stratigraphy and glaciotectonic structures of a relict deformable bed of permafrost at the northwestern margin of the Laurentide Ice Sheet, Tuktoyaktuk Coastlands, Canada. *J. Glaciol.* 50, 399-412.
- Núñez-Betelu, L.K., Hills, L.V., Krause, F.F., 1994. Upper Cretaceous paleoshorelines of the northeastern Sverdrup Basin, Ellesmere Island, Canadian Arctic Archipelago. In: ICAM-94 Proceedings, Stratigraphy and Paleogeography, pp. 43-49.
- O'CoFaigh, C., Evans, D.J.A., England, J., 2003. Ice-marginal terrestrial landsystems: sub-polar glacier margins of the Canadian and Greenland high arctic. In: Evans, D.J.A. (Ed.), *Glacial Landsystems*. Arnold, London, pp. 44-64.
- Pedersen, S.A.S., 1989. Glacitectorite: brecciated sediments and cataclastic sedimentary rocks formed subglacially. In: Goldthwaite, R.P., Matsch, C.L. (Eds.), *Genetic Classification of Glacigenic Deposits*. Balkema, Rotterdam, pp. 89-91.

- Pedersen, S.A.S., 2005. Structural Analysis of the Rubjerg Knude Glaciotectonic Complex, Vendsyssel, Northern Denmark. In: Geological Survey of Denmark and Greenland, Bulletin 8.
- Phillips, E.R., Lee, J.R., Burke, H.F., 2008. Progressive proglacial to subglacial deformation and syntectonic sedimentation at the margins of the Mid-Pleistocene British ice sheet: evidence from north Norfolk, UK. *Quat. Sci. Rev.* 27, 1848-1871.
- Phillips, E., Lee, J.R., Evans, H.M. (Eds.), 2011. *Glaciotectonics e Field Guide*. Quaternary Research Association.
- Phillips, E., Merritt, J., 2008. Evidence for multiphase water-escape during rafting of shelly marine sediments at Clava, Inverness-shire, NE Scotland. *Quat. Sci. Rev.* 27, 988-1011.
- Piotrowski, J.A., 2006. Groundwater under ice sheets and glaciers. In: Knight, P.G. (Ed.), *Glacier Science and Environmental Change*. Blackwell Publishing, Oxford, pp. 50-59.
- Polyak, L., Edwards, M.H., Coakley, B.J., Jakobsson, M., 2001. Ice shelves in the Pleistocene Arctic Ocean inferred from deep-sea glaciogenic scouring. *Nature* 410, 453-459.
- Rijsdijk, K.F., Owen, G., Warren, W.P., McCarroll, D., van der Meer, J.J.M., 1999. Clastic dykes in over-consolidated tills: evidence for subglacial hydrofracturing at Killiney Bay, eastern Ireland. *Sediment. Geol.* 129, 111-126.
- Rotniki, K., 1976. The theoretical basis for and a model of glaciotectonic deformations. *Quaest. Geogr.* 3, 103-139.
- Sharp, M.J., 1985. Sedimentation and stratigraphy at Eyjabakkajökull: an Icelandic surging glacier. *Quat. Res.* 24, 268-284.
- Sharp, M.J., 1988. Surging glaciers: behaviour and mechanisms. *Prog. Phys. Geogr.* 12, 349-370.
- Sugden, D.E., Marchant, D.R., Potter Jr., N., Souchez, R.A., Denton, G.H., Swisher, C.C., Tison, J.L., 1995. Preservation of Miocene glacier ice in East Antarctica. *Nature* 376, 412-414.
- Svendsen, J.I., Alexanderson, H., Astakhov, V.I., 2004. Late Quaternary ice sheet history of Northern Eurasia. *Quat. Sci. Rev.* 23, 1229-1271.
- Taylor, A.E., Dallimore, S.R., Outcalt, S.I., 1996. Late Quaternary history of the Mackenzie-Beaufort region, arctic Canada, from modeling of permafrost temperatures: the onshore-offshore transition. *Can. J. Earth Sci.* 33, 52-61.
- Tozer, E.T., 1956. Geological Reconnaissance of Prince Patrick Island, Eglinton and Western Melville Islands, Arctic Archipelago, Northwest Territories. Geological Survey of Canada, pp. 1-32. Paper. 55-5.
- Tsyvovich, N.A., 1975. *The Mechanics of Frozen Ground*. McGraw-Hill, New York.
- Twiss, R.J., Moores, E.M., 1992. *Structural Geology*. Freeman and Co., New York.
- van der Meer, J.J.M., Kjaer, K.H., Kruger, J., Rabassa, J., Kilfeather, A.A., 2009. Under pressure: clastic dykes in glacial settings. *Quat. Sci. Rev.* 28, 708-720.
- Van der Wateren, F.M., 1995. Structural geology and sedimentology of push moraines. *Meded. Rijks Geol. Dienst* 54.
- Vincent, J.-S., 1982. The Quaternary history of Banks island, northwest territories, Canada. *Geogr. Phys. Quat.* 36, 209-232.
- Vincent, J.-S., 1983. La géologie du quaternaire et la geomorphologie de L'île Banks, arctique Canadien. In: Commission Geologique du Canada Memoir 405.
- Vincent, J.-S., 1984. Quaternary stratigraphy of the western Canadian Arctic archipelago. In: Fulton, R.J. (Ed.), *Quaternary Stratigraphy of Canada e a Canadian Contribution to IGCP Project 24*. Geological Survey of Canada, pp. 87-100, 84-10.
- Vincent, J.-S., 1989. Quaternary geology of the northern Canadian Interior Plains. In: Fulton, R.J. (Ed.), *Quaternary Geology of Canada and Greenland: Geological Survey of Canada, Geology of Canada, 1*, pp. 100-137.
- Vincent, J.-S., 1990. Late Tertiary and early Pleistocene deposits and history of Banks island, southwestern Canadian arctic Archipelago. *Arctic* 43, 339-363.

- Vincent, J.-S., 1992. The Sangamonian and early Wisconsinan glacial record in the western Canadian Arctic. In: Clark, P.U., Lea, P.D. (Eds.), *The Last Glacial interglacial Transition in North America*. Geological Society of America. Special Paper. 270, 233-252.
- Vincent, J.S., Occhietti, S., Rutter, N., Lortie, G., Guilbault, J.-P., De Boutray, B., 1983. The Late Tertiary-Quaternary record of the Duck Hawk bluffs, Banks Island, Canadian Arctic Archipelago. *Can. J. Earth Sci.* 20, 1694-1712.
- Vincent, J.-S., Morris, W.A., Occhietti, S., 1984. Glacial and non-glacial sediments of Matuyama paleomagnetic age on Banks Island, Canadian Arctic Archipelago. *Geology* 12, 139-142.
- Waller, R.I., Murton, J., Whiteman, C., 2009. Geological evidence for subglacial deformation of Pleistocene permafrost. *Proc. Geol. Assoc.* 120, 155-162.
- Waller, R., Phillips, E., Murton, J., Lee, J., Whiteman, C., 2011. Sand intraclasts as evidence of subglacial deformation of Middle Pleistocene permafrost, North Norfolk, UK. *Quat. Sci. Rev.* 168, 673-688.
- Waller, R.I., Murton, J.B., Kristensen, L., 2012. Glacier-permafrost interactions: processes, products and glaciological implications. *Sediment. Geol.* 255-256, 1-28.
- Wintle, A.G., 2010. Future directions of luminescence dating of quartz. *Geochronometria* 37, 1-7.

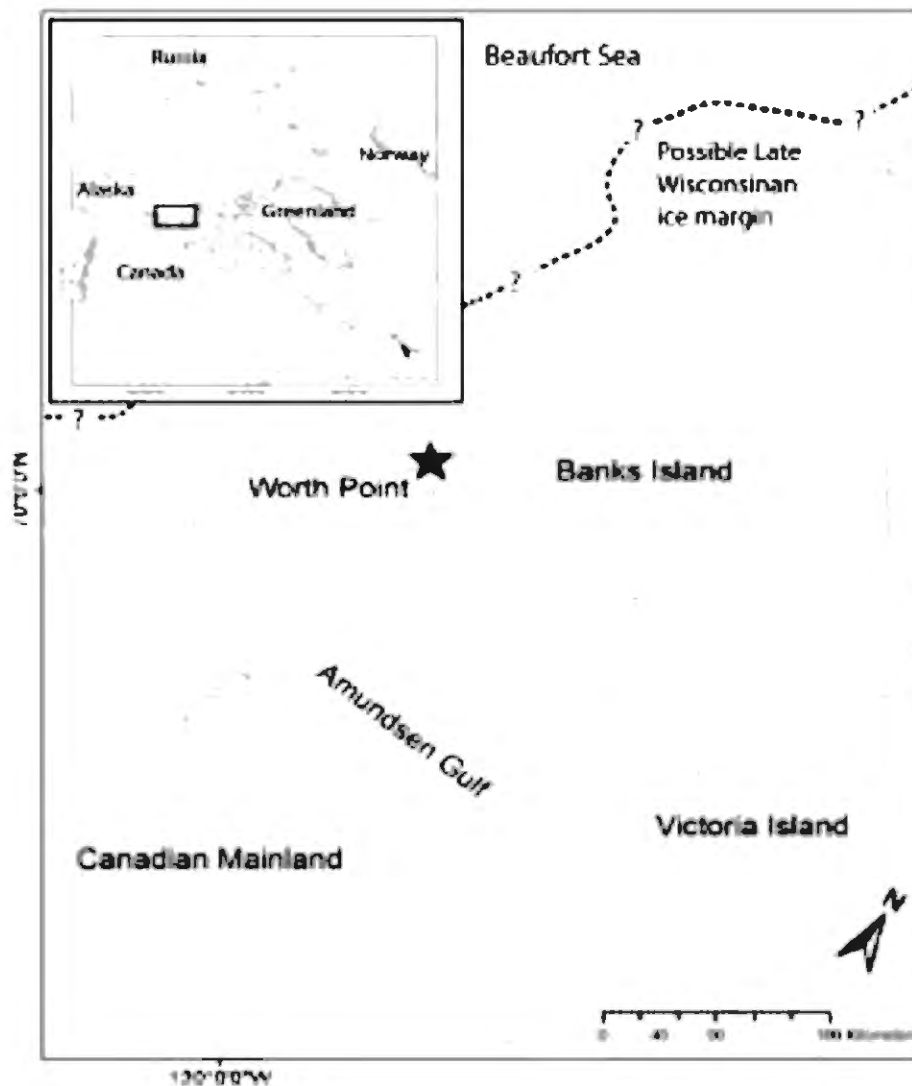


Fig. 1. Location map of Worth Point, Banks Island, western CAA, showing possible Late Wisconsinan ice margin after England et al. (2009), Lakeman and England (2012, 2013) and Vaughan and England (in prep).

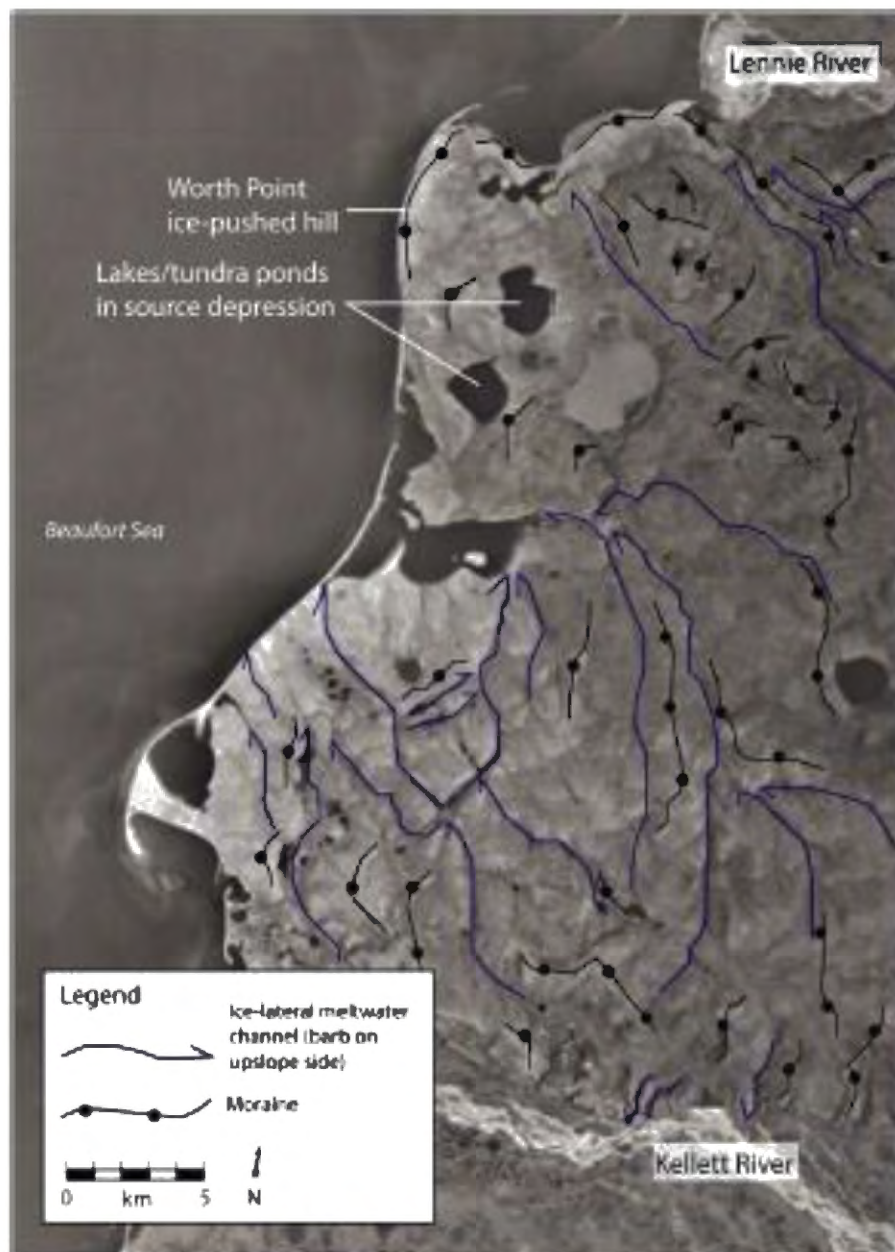


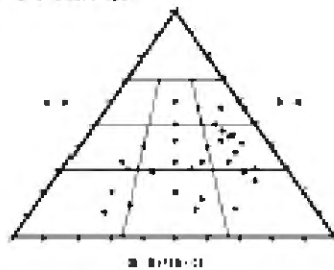
Fig. 2. Aerial photograph of Worth Point showing primary meltwater channels, moraines, and bounding river valleys.



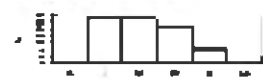
Fig. 3. a: Thermal erosion and undercutting of bluffs leads to frequent detachment of sediment blocks. b: Melt-out of buried glacial ice and ground ice causes widespread slumping and slope failure. c: Heavily brecciated raft comprising distal marine mudstone of the Kk Fm. d: Thrust-faulted raft of ES Fm sandstone and siltstone with typical green and red banding. e: Thrust-faulted raft of Bft Fm composed of well-sorted sand and gravel. f: Glaciomarine diamict displaying crude bedding and containing striated clasts. g: Sub-horizontally bedded and unshifled glaciofluvial sand and gravel. h: Heterogenous and compacted diamict (site for clast fabric analyses). i: Glaciotectonite with large-scale organics and deformed fine-grained matrix (below prominent log). j: Raft of buried glacial ice showing crude bedding and small inclusions melting out. k: Sheet of ground ice occupying a fault/plane of weakness within brecciated Kk Fm. (For interpretation of the references to colour in this figure legend, the reader is referred to the web version of this article)



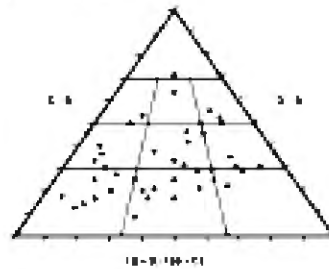
Site 1: LF 6 - class shape



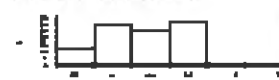
Site 1: LF 6 - class roundness



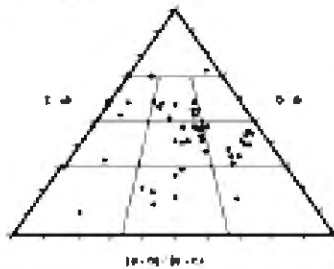
Site 2: LF 6 - class shape



Site 2: LF 6 - class roundness



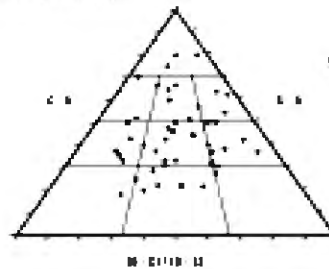
Site 3: LF 3 - class shape



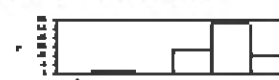
Site 3: LF 3 - class roundness



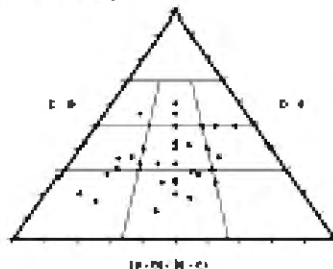
Site 4: LF 5 - class shape



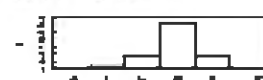
Site 4: LF 5 - class roundness



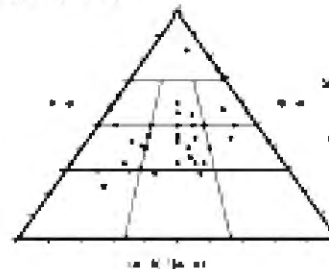
Site 5: LF 5 - class shape



Site 5: LF 5 - class roundness



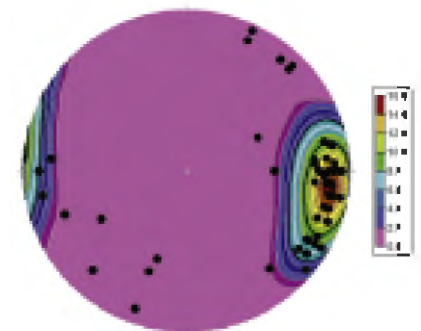
Site 6: LF 9 - class shape



Site 6: LF 9 - class roundness



Site 2: LF 6 - class form



Statistical Summary

Property	Summary	Class Area
Number of Sample Points	35	
Mean Lineation Azimuth	92.8	
Mean Lineation Plunge	11.4	
Great Circle Azimuth	10.0	
Great Circle Plunge	15.5	
1st Eigenvalue	2.146	
2nd Eigenvalue	0.184	
3rd Eigenvalue	0.00	
U1 (E1 - E2)	1.962	
U1 (E1 - E3)	1.777	
U1 (E2 - E3)	1.42	
Spherical Variance	0.3443	
Phi	0.6657	

Fig. 4. Class form analyses based on data collected from two separate and representative sites for LF 3, LF 5 and LF 6. Class fabric analyses shown for site 2 for LF 6.

Simplified Worth Point Tectonostratigraphy

0.1 km

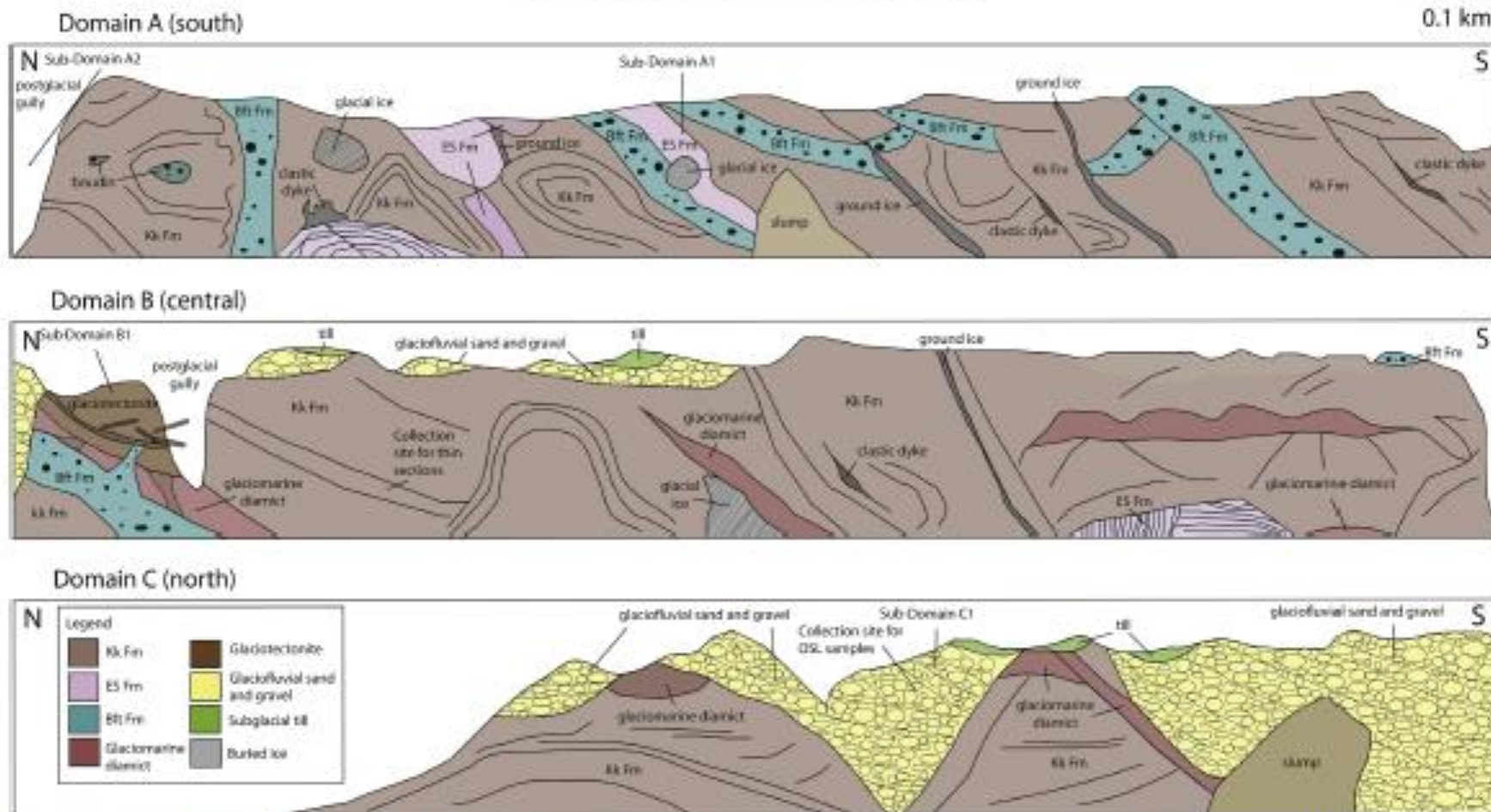


Fig. 5. Simplified tectonostratigraphy of Worth Point along a ~6 km north-south transect (as observed from the coast). Domain A forms the southernmost ~2 km, Domain B forms the central ~2.2 km, and Domain C forms the northernmost ~1.8 km of the coastal section. Detailed deformation stratigraphies and styles are not shown as they are too numerous and complex to include at this scale. Readers should use the gully as a reference to orient themselves through the paper and to note the primary locations of lithofacies and their dominant tectonostratigraphic settings. Section localities described in the paper are identified, along with sample collection sites for OSL dating and thin section analysis.

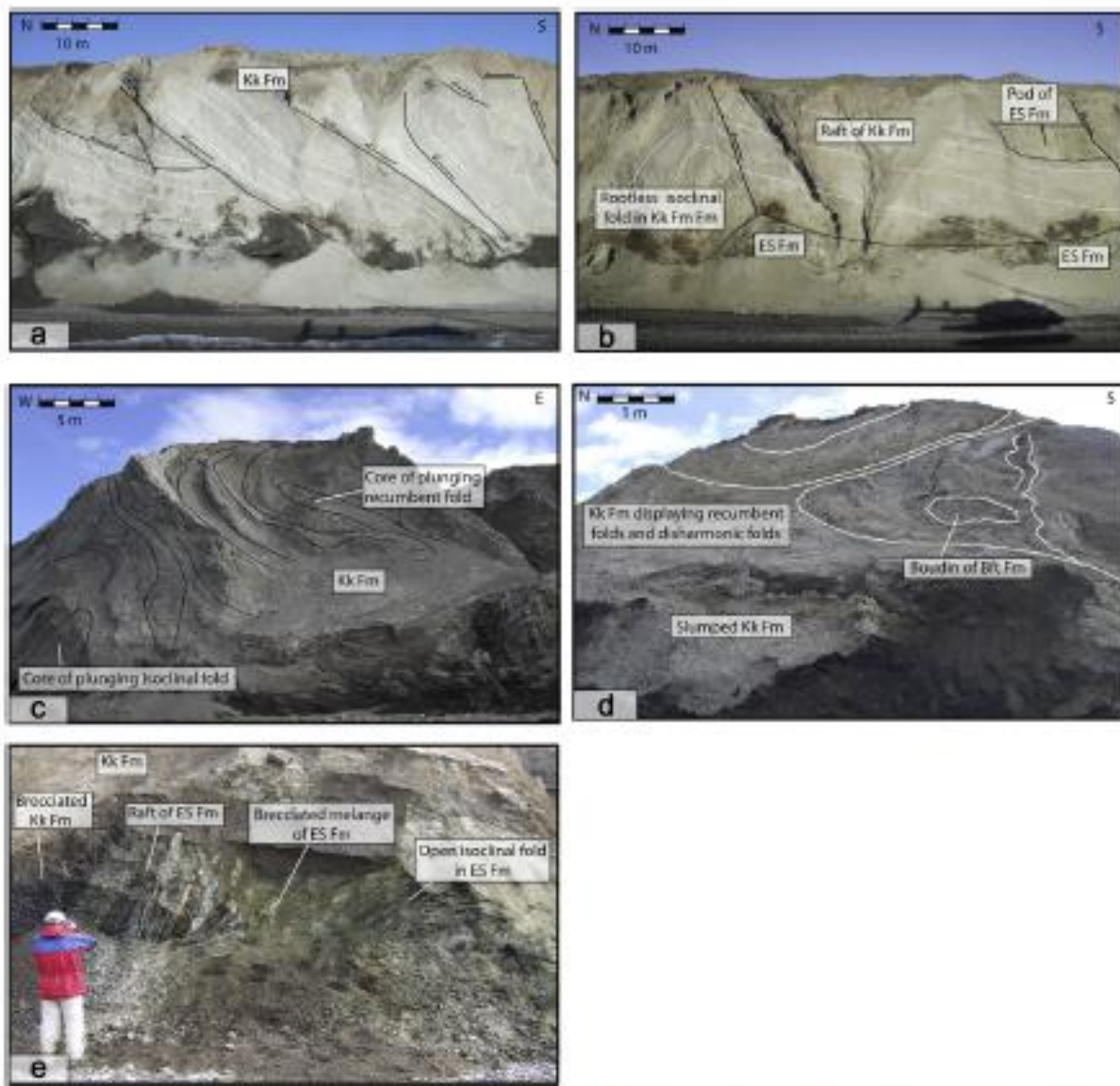


Fig. 6. Figures demonstrate large-scale tectonic architecture and common deformation structures. **a:** Imbricated thrust-faulted rafts of Kk Fm orientated to the SE (toward source basin) truncated by low-angle thrust faults near the modern surface. **b:** Thrust-faulted Kk Fm with rootless isoclinal fold and coherent pod of ES Fm. Thrust-faulted raft of ES Fm at base. **c:** Core of recumbent fold and plunging isoclinal fold in Kk Fm. **d:** Fold interference in Kk Fm with boudin of Bfm at core of a recumbent fold. **e:** Brittle and ductile deformation of ES Fm. Open isoclinal fold in ES Fm (right) truncated by back-thrust high-angle raft of ES Fm with brecciated shear zones either side of the raft (left).

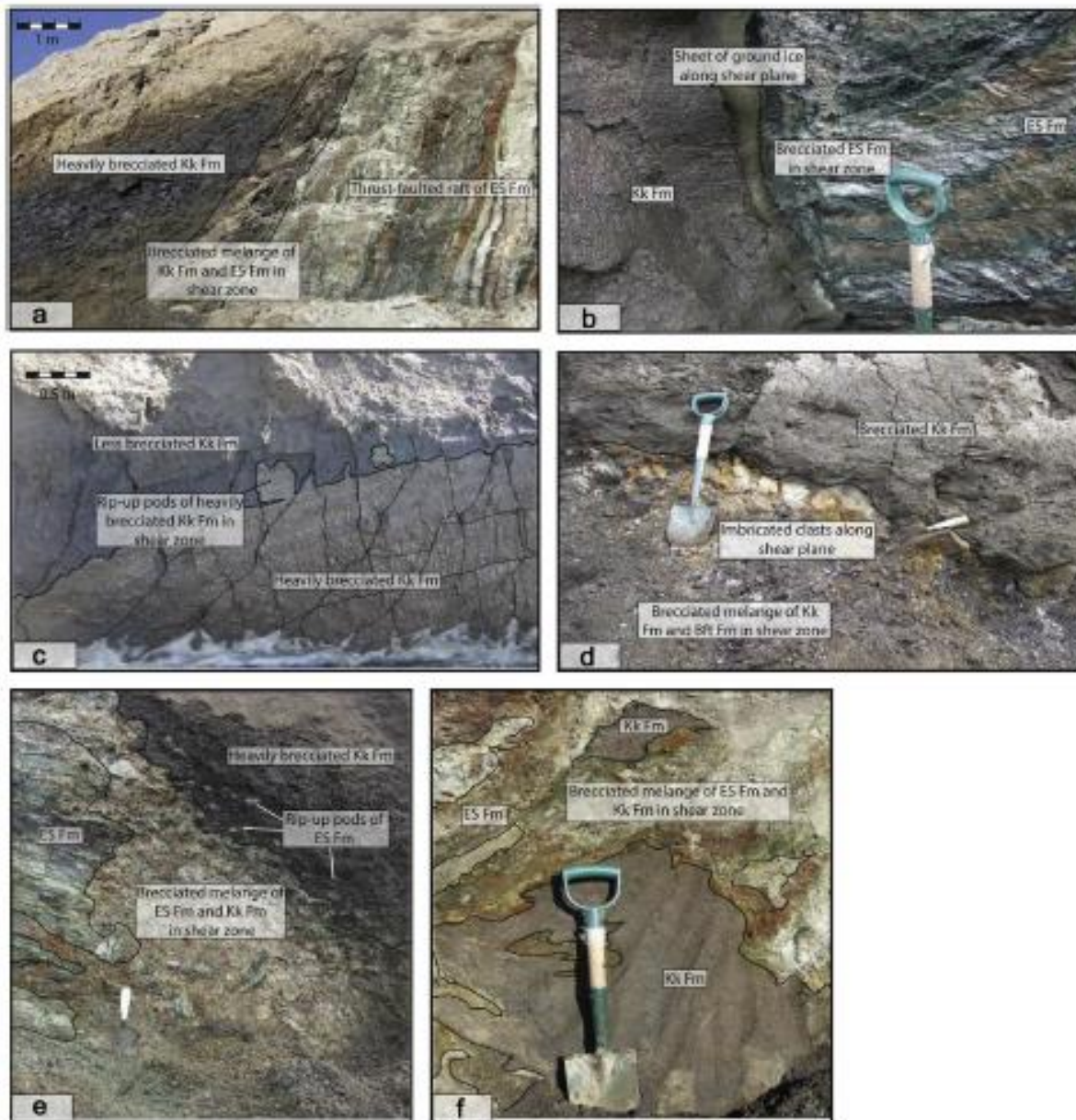


Fig. 7. a: Brecciated melange in shear zone between thrust-faulted rafts of ES Fm (to right) and brecciated Kk Fm (to left). **b:** Brecciated shear zone between ES Fm (right) and Kk Fm (left) with ground ice occupying shear plane. **c:** Rip-up at shear zone between two differentially brecciated rafts of Kk Fm. **d:** Imbricated clasts along shear plane between Kk Fm (above) and brecciated melange of Kk Fm and Bft Fm (below). **e:** Intensely brecciated ES Fm (left) and Kk Fm (right) in shear zone between thrust rafts of ES Fm and Kk Fm. **f:** Rip-up pods of Kk Fm and ES Fm (melange) in a shear zone between Kk Fm and ES Fm.

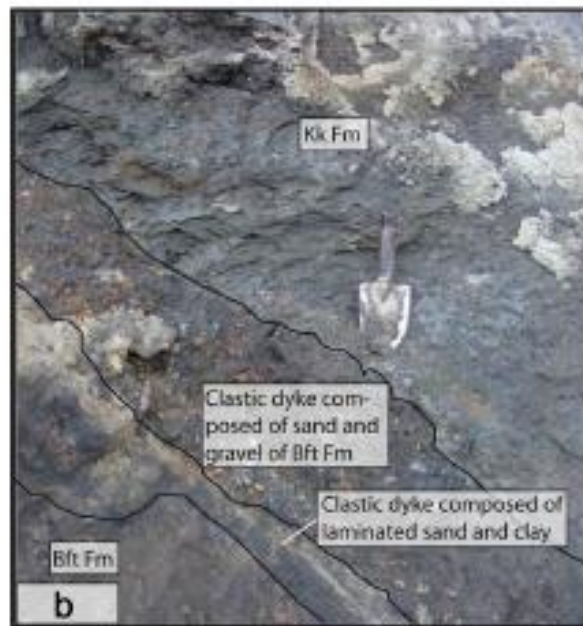
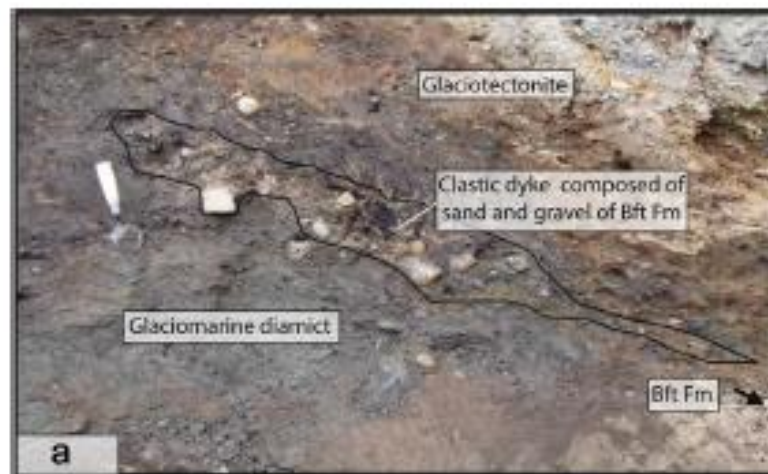


Fig. 8. a: Clastic dyke composed of massive sand and gravel sourced from an underlying raft of Bft Fm. The clastic dyke has been injected under high hydraulic pressure along a shear plane separating glaciomarine diamict and glaciotectonite. **b:** Multi-phase clastic dyke. Lower clastic dyke is composed of laminated sand and clay (sourced from the underlying Bft Fm and Kk Fm) and records a period of lower, more variable hydraulic pressures. Upper dyke is composed of massive sand and gravel (sourced from the underlying Bft Fm) and clearly cross-cuts the lower dyke. The upper dyke records a subsequent period of higher hydraulic pressures. The same shear plane has been utilized twice for hydrofracturing. **c:** Forking clastic dyke composed of massive and laminated clay injected into glaciomarine diamict under lower hydraulic pressures.

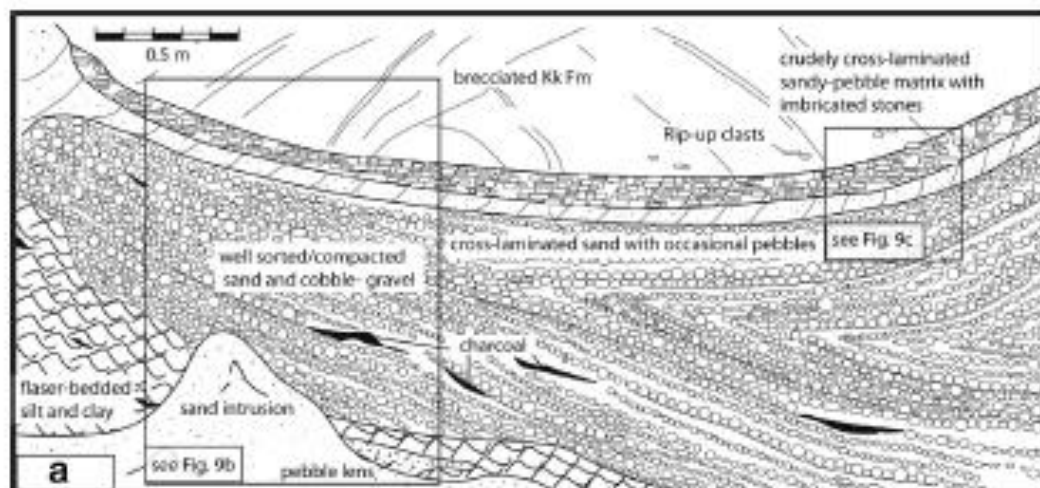


Fig. 9. a: Scaled log of Domain A1. Reverse-faulted raft of ES Fm comprising flaser-bedded silt and clay, well-sorted crudely bedded cobble-gravel with charcoal inclusions, cross-laminated sand and pebbles, and crudely cross-laminated sandy-pebbles with imbricated stones. ES Fm raft is overlain by a raft of brecciated Kk Fm. **b:** Excellent preservation of depositional structures within the raft of ES Fm. **c:** Close-up of sharp fault surface separating raft of ES Fm and overlying raft of brecciated Kk Fm. **d:** Buried glacial ice with debris-rich bands currently melting out of section base where it comprises isolated bodies at the contact between raft of ES Fm and underlying raft of Bft Fm. Debris melting out of glacial ice includes granules and coal directly sourced from the overlying ES Fm.

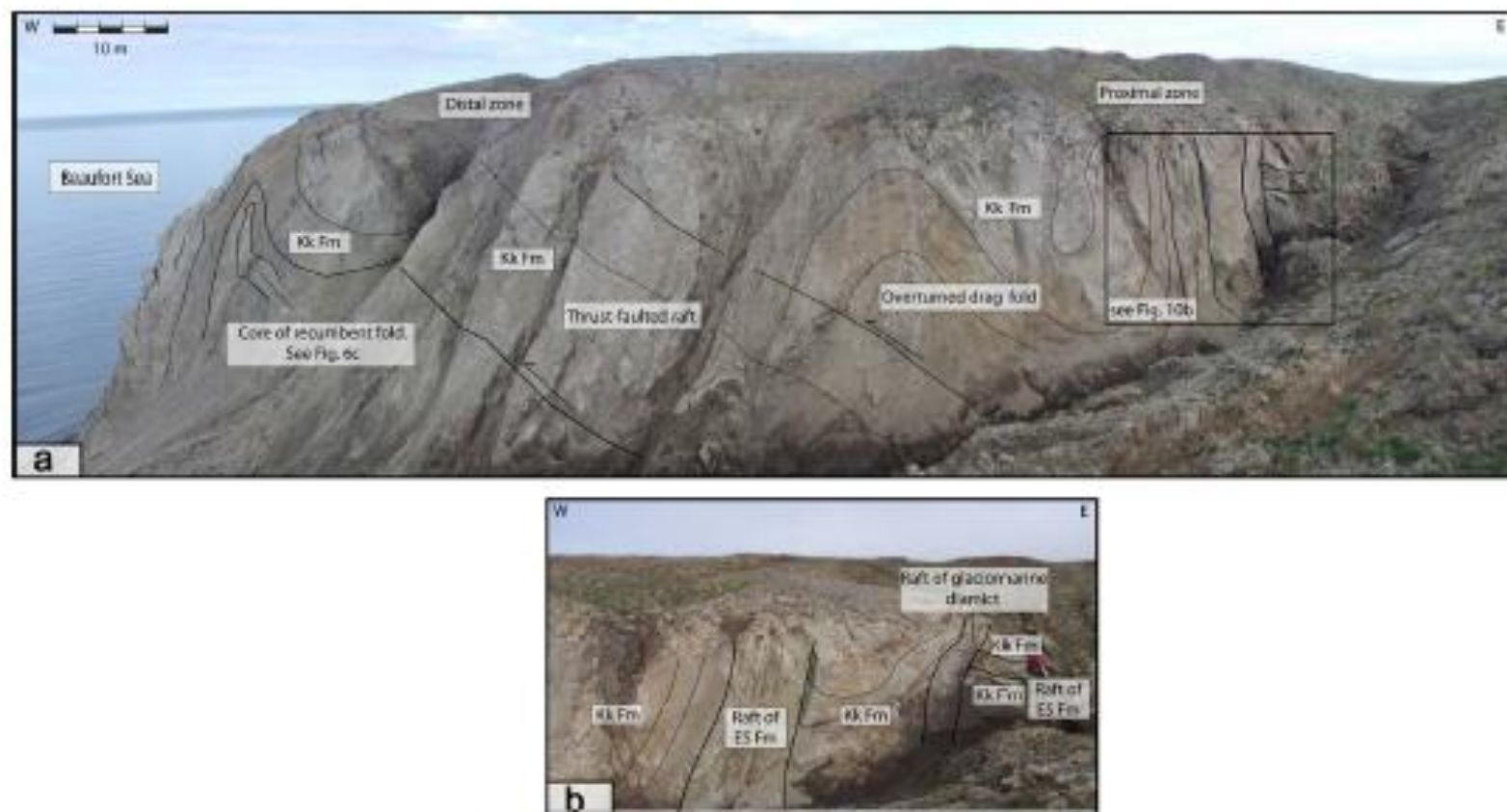


Fig. 10. a: Panorama showing an east–west exposure (across-strike) of Domain A2, dominated by Kk Fm. A distinct change in deformation can be observed from east (back-thrusted and thrust-faulted bedrock rafts) to west (large-scale recumbent fold). **b:** Close-up of easternmost stratigraphy showing low-angle thrust-faulted rafts of Kk Fm and ES Fm that have been truncated by imbricately stacked back-thrusted rafts of glaciomarine diamict, Kk Fm, and ES Fm.

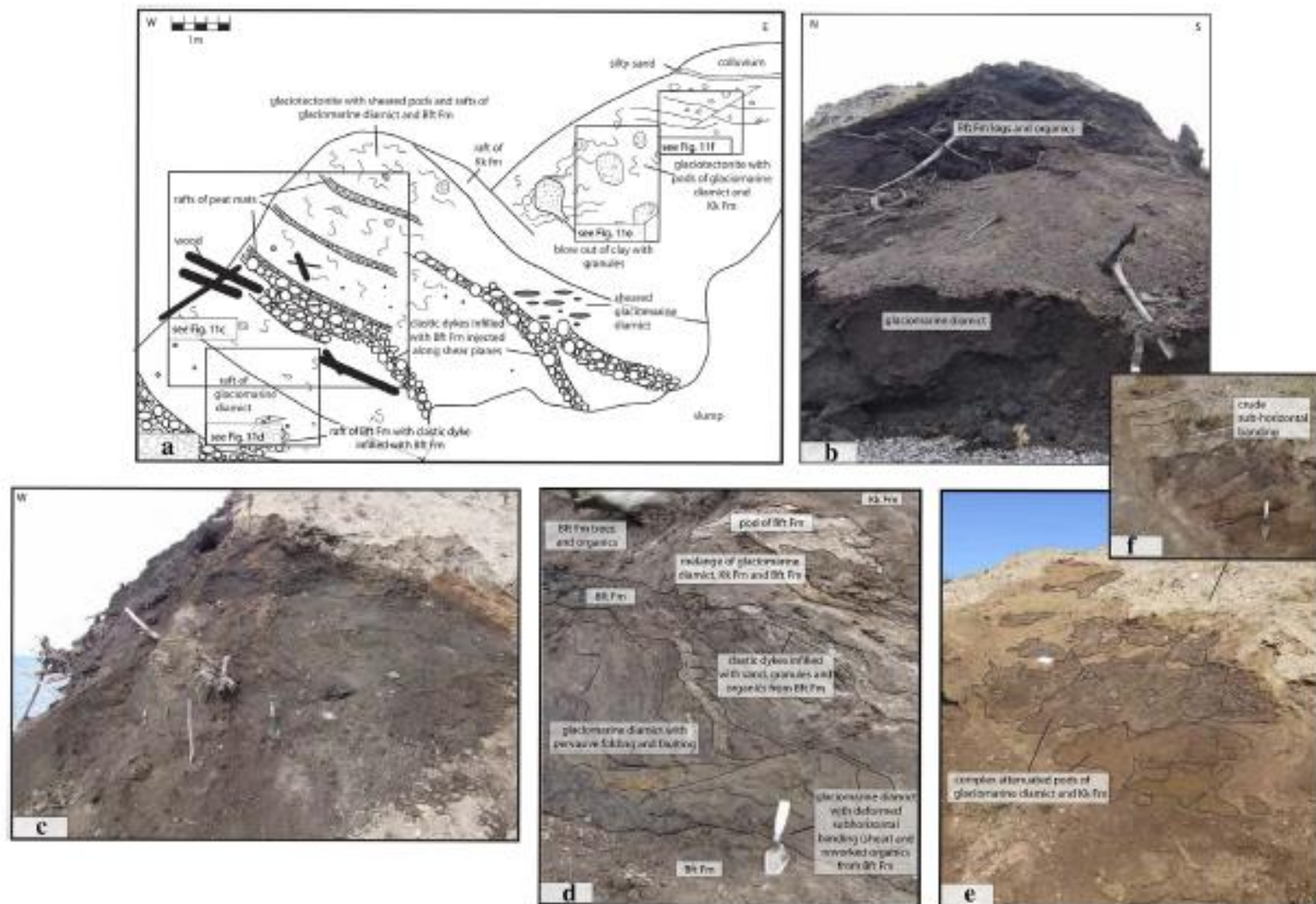


Fig. 11. a: Scaled log of Domain B1 (west–east). Basal raft of Bft Fm overlain by a raft of glaciomarine diamict, in turn overlain by a complex glaciotectonite melange. From base upward, melange comprises three organic rafts sourced from the Bft Fm that have been sheared and deformed along with rafts of glaciomarine diamict and Kk Fm. Glaciotectonite becomes increasingly homogenous up-section as Bft Fm organics become absent and Kk Fm and glaciomarine diamict dominate. The deformed Kk Fm and glaciotectonite display progressively more distinct strain banding with distance up-section. b: B1 section as it appears from the coast (north-south). Logs and peat eroding out of basal organic raft are inconspicuous. c: Base of glaciotectonite melange showing logs eroding out of basal organic raft. d: Close-up of glaciotectonite melange at base of sequence. Note pervasive folding, small-scale faults, detached pods of Bft Fm, and large-scale organics. e: Close-up of glaciotectonite melange further up-section. Note absence of large-scale organics, and complex attenuation of glaciomarine diamict and Kk Fm. f: Close-up of glaciotectonite melange at top of section. Note crude sub-horizontal banding.

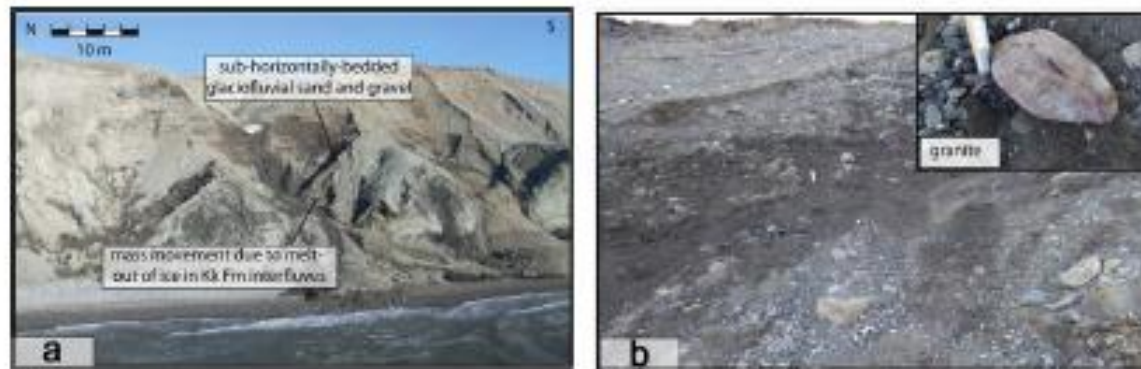


Fig. 12. a: Sub-horizontally bedded glaciofluvial sand and gravel incising into Kk Fm (interfluvies currently slumping), b: Close-up of coarse glaciofluvial sand and gravel displaying sub-horizontal bedding and containing occasional granite clasts (inset).

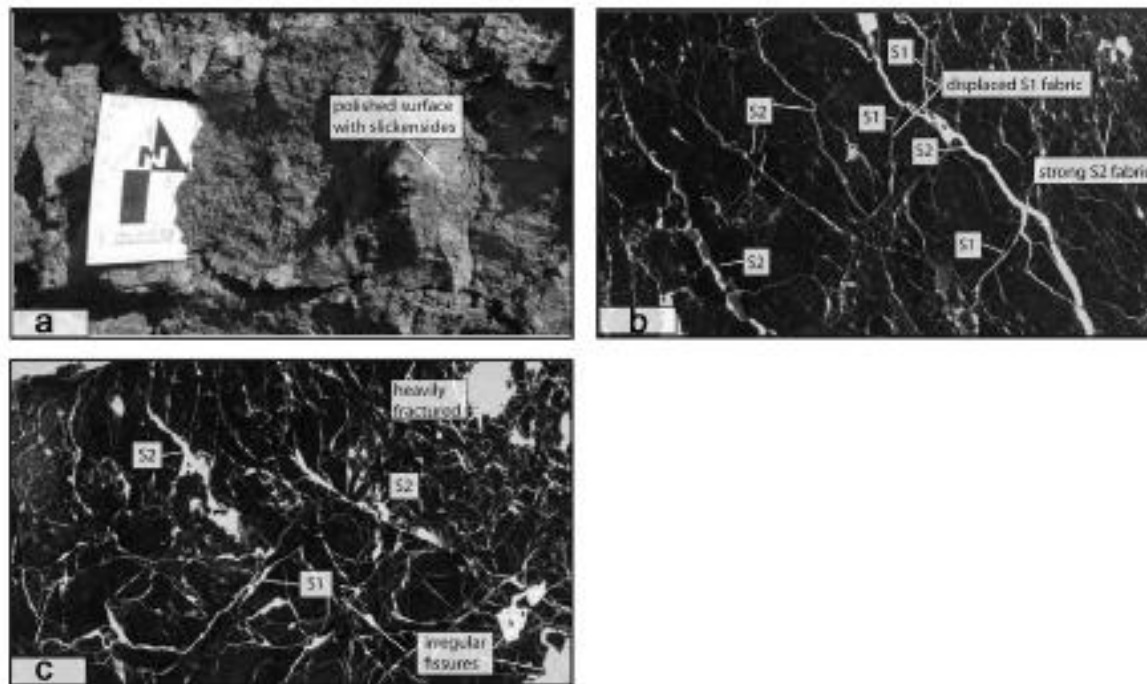
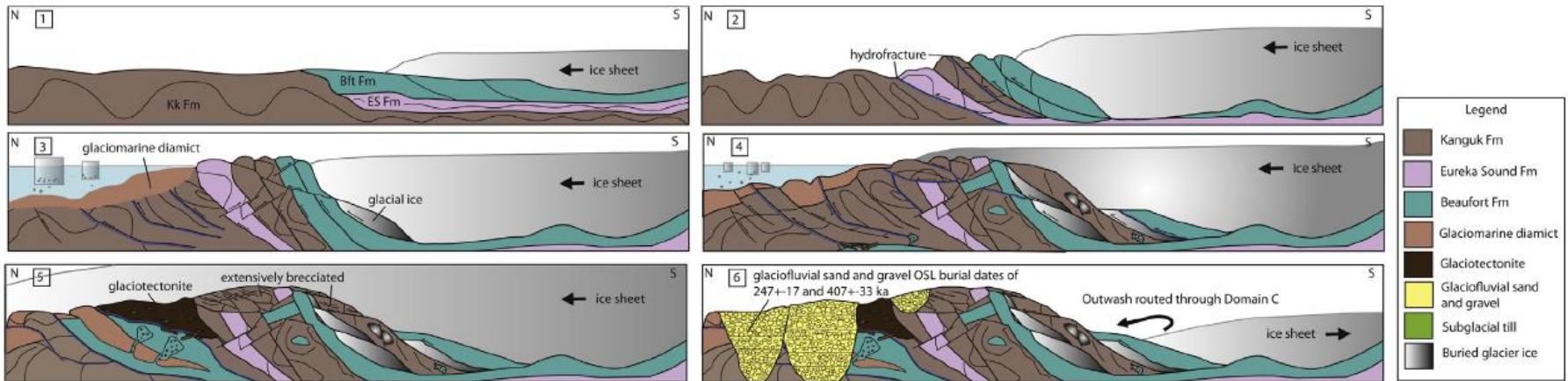


Fig. 13. a: Close-up of brecciated Kk Fm where sediment samples were collected for thin section production. Kk Fm displays polished surfaces and slickensides. b: Thin section of sample 1 of brecciated Kk Fm. c: Thin section of sample 2 of brecciated Kk Fm.

Glaciotectonic Model for the Worth Point stratigraphic sequence

Glaciotectonic event 1: Ice-marginal deformation, glaciomarine reworking, and subglacial deformation



Glaciotectonic event 2: Subglacial deformation

Postglacial erosion to produce modern bluffs

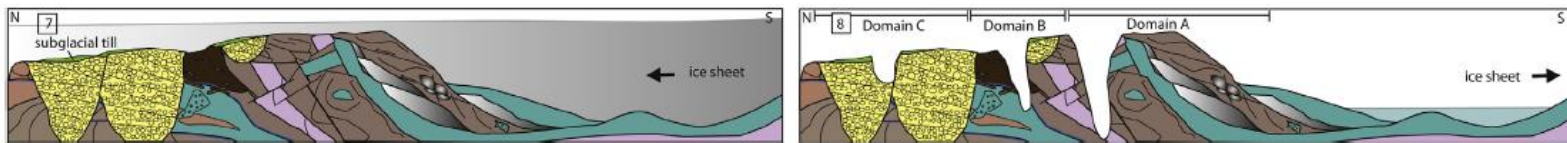


Fig. 14. Simplified, schematic two-dimensional glaciotectonic model showing the progressive evolution of the Worth Point stratigraphic sequence. The model shows the evolution of the stratigraphic sequence during two distinct glaciotectonic events. Each glaciotectonic event is broken into blocks (1–8) that represent key snapshots in time when the stratigraphic sequence underwent major modification. Block 8 shows a simplified diagram of the stratigraphic sequence as it looks today, with the approximate locations of Domains A–C. The model shows strata oriented south–north (i.e. observed from the coast) with ice advance from the southeast during glaciotectonic event 1, and ice advance from the east during glaciotectonic event 2. As a result, deformational patterns and structures shown for glaciotectonic event 1 are the result of glacially-imposed compression and shear oriented oblique to the viewer, and during glaciotectonic event 2 perpendicular to the viewer. *Glaciotectonic event 1* is represented by blocks 1–6. Blocks 1–2 show initial compressional deformation of the Early Cretaceous and Late Tertiary bedrock by progressive ice-marginal advance, while block 3 shows the concurrent reworking of strata by a glaciomarine transgression and the deposition of a glaciomarine diamict. Compressional deformation was most intense proximal to the ice-margin and best represented in Domain A. Blocks 4–5 show a readvance or sustained advance of the ice sheet and the overriding of the previously deformed strata. This overriding led to the overprinting of shear deformation structures and the deposition of a glaciotectonite that are best represented in Domain B. Block 6 shows subsequent ice sheet retreat, and the incision and aggradation (dated to ~247 and ~407 ka BP) of outwash valleys in Domain C. A deglacial marine regression (to facilitate incision) and transgression (to facilitate aggradation) are inferred. *Glaciotectonic event 2* is represented by block 7. Block 7 shows the overriding of strata by an ice sheet that produced minimal deformation and deposited a capping till. The till and deformed strata are best preserved and characterised in Domain C. The model shows how each glaciotectonic event affected the entire stratigraphic sequence, with the final tectonostratigraphy (block 8) resulting from polydeformation. However, the model also highlights how Domains A–C display deformational patterns and structures resulting from each glaciotectonic event to varying extents. Ice-marginal deformation during glaciotectonic event 1 is best displayed in Domain A, subglacial deformation during glaciotectonic event 1 is best displayed in Domain B, and subglacial deformation during glaciotectonic event 2 is best displayed in Domain C.